duced by the addition of tacrolimus but not CyA. Thus, tacrolimus protected the mitochondrial respiratory chain complex 1 function from the impact of the core protein, decreased oxidative stress, and improved steatosis and insulin resistance.

Some of features induced by the core protein including steatosis, insulin, and DNA damage were already present in the core gene transgenic mice at 3 months of age as the baseline, and those were improved by tacrolimus treatment. This fact indicates that tacrolimus is not only preventing the development of core-induced features but also reversing such changes in the mouse liver.

The tacrolimus dose used in the current study was 0.1 mg/kg b.wt. This is the same dose as that used in recipients of liver or kidney transplantation. The result of a subexperiment with a lower tacrolimus dose of 0.02 mg/kg b.wt. was similar to that with the dose of 0.1 mg/kg b.wt. This finding is promising because it indicates that the "anti-core protein effect" may be achievable at such a low dose of tacrolimus without provoking strong immunosuppression. The tacrolimus concentration (100 nmol/L) that caused the anti-core protein effect in the cultured cell study is similar to that in the blood of recipients of liver transplantation and much lower than those used in previous studies.[19,38] In the current study, tacrolimus was administered only i.p., although it tacrolimus is administered i.v. or p.o. in humans. Therefore, a concern may arise regarding the administration route. Because the bioavailability of tacrolimus is approximately 25% (range from 5 to 93%) in human patients,[39] a difference in the concentrations of tacrolimus may be possible between i.p. and p.o. administration. However, in human patients, target levels of tacrolimus concentration are generally achieved by p.o. administration as the maintenance therapy. Therefore, the target concentration would be achieved in mouse models by p.o. administration for 3 months as it is in human patients. Our current results strongly support the notion that tacrolimus can protect the mitochondrial respiratory function, resulting in a reduction of ROS production.

There is also a controversy concerning the effect of tacrolimus on glucose homeostasis. Post-transplantation diabetes is a complication in kidney or liver transplantation.[40,41] *In vivo* and *in vitro* studies have shown that tacrolimus may inhibit insulin secretion from the pancreatic β-cells.[40] Thus, tacrolimus may have a potential to induce diabetes. However, there have been no well designed studies on this specific point: in one study, corticosteroid withdrawal from tacrolimus-based immunosuppression reduced insulin resistance without changing insulin secretion.[41] In our study using the HCV mouse model, tacrolimus administration at the dose similar to those in organ transplant recipients decreased serum insulin levels without increasing plasma glucose levels. These results point toward the future use of tacrolimus *in vivo* for the amendment of metabolic abnormalities, such as steatosis and insulin resistance, associated with HCV infection. However, it should be noted that there is a difference between our mouse model and human patients. Organ transplant recipients generally have injury to other bodily organs after a prolonged course of illness, whereas the mouse model we have exploited does not. In addition, our mouse model originally has insulin resistance with the presence of hyperplasia of Langerhans islands.[16] Therefore, the effect of tacrolimus on glucose homeostasis in the current mouse study may not be exactly applicable to human patients.

The results of the gene expression analysis by microarray and subsequent real-time PCR were of considerable interest. Tacrolimus reduced the mRNA levels of TNF-α, SCD-1, and SREBP-1c genes, which are elevated in both patients with chronic hepatitis C and HCV core gene transgenic mice.[30,31] The elevation in the TNF-α level causes insulin resistance *in vivo*, which is also observed in HCV core gene transgenic mice.[16] The elevations in SREBP-1c and SCD-1 gene mRNA levels cause the overproduction of triglycerides, leading to the development of steatosis. The reductions in the expression levels of these genes may explain the effect of tacrolimus on the improvement of steatosis, insulin resistance, and oxidative stress in these HCV models. Although recent investigations have shown that the immunosuppressive drugs tacrolimus and rapamycin inhibit the expression of different inflammatory mediators,[42,43] the anti-inflammatory functions of these drugs are not well established. Our *in vitro* and *in vivo* experiments confirmed that tacrolimus inhibited the induction of ROS generation, which is mediated by the core protein. Our data indicate that the inhibition of ROS formation may explain part of the favorable effect of immunosuppressive agents on inflammatory conditions.

In conclusion, our results demonstrate that tacrolimus has protective potential against damage caused by the HCV core protein including the induction of steatosis, insulin resistance, and oxidative stress, both in mice and cultured cells. Although more studies are required to elucidate the precise mechanism underlying the potential of tacrolimus in reversing the pathogenesis in HCV infection, these results may provide new therapeutic tools for chronic hepatitis C, in which oxidative stress and abnormalities in lipid and glucose metabolism contribute to liver pathogenesis.

References

1. Saito I, Miyamura T, Ohbayashi A, Harada H, Katayama T, Kikuchi S, Watanabe Y, Koi S, Onji M, Ohta Y, Choo Q, Houghton M, Kuo G: Hepatitis C virus infection is associated with the development of hepatocellular carcinoma. Proc Natl Acad Sci USA 1990, 87:6547–6549
2. Simonetti RG, Camma C, Fiorello F, Cottone M, Rapicetta M, Marino L, Fiorentino G, Craxì A, Ciccaglione A, Giuseppetti R, Stroffolini T, Pagliaro L: Hepatitis C virus infection as a risk factor for hepatocellular carcinoma in patients with cirrhosis. Ann Intern Med 1992, 116:97–102
3. Scheuer PJ, Ashrafzadeh P, Sherlock S, Brown D, Dusheiko GM: The pathology of chronic hepatitis C. Hepatology 1992, 15:567–571
4. Bach N, Thung SN, Schaffner F: The histological features of chronic hepatitis C and autoimmune chronic hepatitis: a comparative analysis. Hepatology 1992, 15:572–577
5. Barba G, Harper F, Harada T, Kohara M, Goulinet S, Matsuura Y, Eder G, Schaff Z, Chapman MJ, Miyamura T, Bréchot C: Hepatitis C virus core protein shows a cytoplasmic localization and associates to cellular lipid storage droplets. Proc Natl Acad Sci USA 1997, 94:1200–1205
6. Moriya K, Yotsuyanagi H, Shintani Y, Fujie H, Ishibashi K, Matsuura Y, Miyamura T, Koike K: Hepatitis C virus core protein induces hepatic steatosis in transgenic mice. J Gen Virol 1997, 78:1527–1531

7. Lerat H, Honda M, Beard MR, Loesch K, Sun J, Yang Y, Okuda M, Gosert R, Xiao SY, Weinman SA, Lemon SM: Steatosis and liver cancer in transgenic mice expressing the structural and nonstructural proteins of hepatitis C virus. Gastroenterology 2002, 122:352–365
8. Caronia S, Taylor K, Pagliaro L, Carr C, Palazzo U, Petrik J, O'Rahilly S, Shore S, Tom BD, Alexander GJ: Further evidence for an association between non-insulin-dependent diabetes mellitus and chronic hepatitis C virus infection. Hepatology 1999, 30:1059–1063
9. Mehta SH, Brancati FL, Sulkowski MS, Strathdee SA, Szklo M, Thomas DL: Prevalence of type 2 diabetes mellitus among persons with hepatitis C virus infection in the United States. Ann Intern Med 2000, 133:592–599
10. Choi J, Ou JH: Mechanisms of liver injury. III. Oxidative stress in the pathogenesis of hepatitis C virus. Am J Physiol Gastrointest Liver Physiol 2006, 290:G847–G851
11. Koike K, Miyoshi H: Oxidative stress and hepatitis C viral infection. Hepatol Res 2006, 34:65–76
12. Korenaga M, Wang T, Li Y, Showalter LA, Chan T, Sun J, Weinman SA: Hepatitis C virus core protein inhibits mitochondrial electron transport and increases reactive oxygen species (ROS) production. J Biol Chem 2005, 280:37481–37488
13. Moriya K, Nakagawa K, Santa T, Shintani Y, Fujie H, Miyoshi H, Tsutsumi T, Miyazawa T, Ishibashi K, Horie T, Imai K, Miyamura T, Kimura S, Koike K: Oxidative stress in the absence of inflammation in a mouse model for hepatitis C virus-associated hepatocarcinogenesis. Cancer Res 2001, 61:4365–4370
14. Moriya K, Fujie H, Shintani Y, Yotsuyanagi H, Tsutsumi T, Matsuura Y, Kimura S, Miyamura T, Koike K: The core protein of hepatitis C virus induces hepatocellular carcinoma in transgenic mice. Nat Med 1998, 4:1065–1067
15. Moriya K, Todoroki T, Tsutsumi T, Yotsuyanagi H, Tsutsumi T, Ishibashi K, Takayama T, Makuuchi M, Watanabe K, Miyamura T, Kimura S, Koike K: Increase in the concentration of carbon 18 monounsaturated fatty acids in the liver with hepatitis C: analysis in transgenic mice and humans. Biophys Biochem Res Commun 2001, 281:1207–1212
16. Shintani Y, Fujie H, Miyoshi H, Tsutsumi T, Kimura S, Moriya K, Koike K: Hepatitis C virus and diabetes: direct involvement of the virus in the development of insulin resistance. Gastroenterology 2004, 126:840–848
17. Piccoli C, Scrima R, Quarato G, D'Aprile A, Ripoli M, Lecce L, Boffoli D, Moradpour D, Capitanio N: Hepatitis C virus protein expression causes calcium-mediated mitochondrial bioenergetic dysfunction and nitro-oxidative stress. Hepatology 2007, 46:58–65
18. Cetinkale O, Konukoğlu D, Senel O, Kemerli GD, Yazar S: Modulating the functions of neutrophils and lipid peroxidation by FK506 in a rat model of thermal injury. Burns 1999, 25:105–112
19. Kaibori M, Inoue T, Tu W, Oda M, Kwon AH, Kamiyama Y, Okumura T: FK506, but not cyclosporin A, prevents mitochondrial dysfunction during hypoxia in rat hepatocytes. Life Sci 2001, 69:17–26
20. Keswani SC, Chander B, Hasan C, Griffin JW, McArthur JC, Hoke A: FK506 is neuroprotective in a model of antiretroviral toxic neuropathy. Ann Neurol 2003, 53:57–64
21. Kaymaz M, Emmez H, Bukan N, Dursun A, Kurt G, Paçsaoğlu H, Paçsaoğlu A: Effectiveness of FK506 on lipid peroxidation in the spinal cord following experimental traumatic injury. Spinal Cord 2005, 43:22–26
22. Ruggieri A, Murdolo M, Harada T, Miyamura T, Rapicetta M: Cell cycle perturbation in a human hepatoblastoma cell line constitutively expressing hepatitis C virus core protein. Arch Virol 2004, 149:61–74
23. Aizaki H, Harada T, Otsuka M, Seki N, Matsuda M, Li YW, Kawakami H, Matsuura Y, Miyamura T, Suzuki T: Expression profiling of liver cell lines expressing entire or parts of hepatitis C virus open reading frame. Hepatology 2002, 36:1431–1438
24. Todoroki T, Imai K, Matsumoto K, Kano S: Initial deactivation of Florisil adsorbent for column chromatographic separation of lipids. Analyst 1983, 108:1267–1269
25. Morrison WR, Smith LM: Preparation of fatty acid methyl esters and dimethylacetals from lipids with boron fluoride-methanol. J Lipid Res 1964, 5:600–608
26. Gelasco AK, Raymond JR: Indoxyl sulfate induces complex redox alterations in mesangial cells. Am J Physiol Renal Physiol 2006, 290:F1551–F1558
27. Williamson DH, Mellanby J, Krebs HA: Enzymic determination of D(−)-β-hydroxybutyric acid and acetoacetic acid in blood. Biochem J 1962, 82:90–96
28. Choi Y, Park Y, Pariza MW, Ntambi JM: Regulation of stearoyl-CoA desaturase activity by the *trans*-10,*cis*-12 isomer of conjugated linoleic acid in HepG2 cells. Biochem Biophys Res Commun 2001, 284:689–693
29. Williamson DH, Lund P, Krebs HA: The redox state of free nicotinamide-adenine dinucleotide in the cytoplasm and mitochondria of rat liver. Biochem J 1967, 103:514–527
30. Tsutsumi T, Suzuki T, Moriya K, Yotsuyanagi H, Shintani Y, Fujie H, Matsuura Y, Kimura S, Koike K, Miyamura T: Intrahepatic cytokine expression and AP-1 activation in mice transgenic for hepatitis C virus core protein. Virology 2002, 304:415–424
31. Moriishi K, Mochizuki R, Moriya K, Miyamoto H, Mori Y, Abe T, Murata S, Tanaka K, Suzuki T, Miyamura T, Koike K, Matsuura Y: Critical role of PA28γ in hepatitis C virus-associated steatogenesis and hepatocarcinogenesis. Proc Natl Acad Sci USA 2007, 104:1661–1666
32. Hoofnagle JH, Seeff LB: Peginterferon and ribavirin for chronic hepatitis C. N Engl J Med 2006, 355:2444–2451
33. Koike K: Antiviral treatment of hepatitis C: present status and future prospects. J Infect Chemother 2006, 12:227–232
34. Adinolfi LE, Gambardella M, Andreana A, Tripodi MF, Utili R, Ruggiero G: Steatosis accelerates the progression of liver damage of chronic hepatitis C patients and correlates with specific HCV genotype and visceral obesity. Hepatology 2001, 33:1358–1364
35. Patton HM, Patel K, Behling C, Tripodi MF, Utili R, Ruggiero G: The impact of steatosis on disease progression and early and sustained treatment response in chronic hepatitis C patients. J Hepatol 2004, 40:484–490
36. Hui JM, Sud A, Farrell GC, Bandara P, Byth K, Kench JG, McCaughan GW, George J: Insulin resistance is associated with chronic hepatitis C virus infection and fibrosis progression. Gastroenterology 2003, 125:1695–1704
37. Hickman IJ, Powell EE, Prins JB, Clouston AD, Ash S, Purdie DM, Jonsson JR: Insulin resistance is associated with chronic hepatitis C and virus infection fibrosis progression. J Hepatol 2003, 39:1042–1048
38. Han SY, Chang EJ, Choi HJ, Kwak CS, Suh SI, Bae JH, Park SB, Kim HC, Mun KC: Effect of tacrolimus on the production of oxygen free radicals in hepatic mitochondria. Transplant Proc 2006, 38:2242–2243
39. Staatz CE, Tett SE: Clinical pharmacokinetics and pharmacodynamics of tacrolimus in solid organ transplantation. Clin Pharmacokinet 2004, 43:623–653
40. Penfornis A, Kury-Paulin S: Immunosuppressive drug-induced diabetes. Diabetes Metab 2006, 32:539–546
41. van Hooff JP, Christiaans MH, van Duijnhoven EM: Evaluating mechanisms of post-transplant diabetes mellitus: Nephrol Dial Transplant 2004, 19(Suppl 6):vi8–vi12
42. Vigil SV, de Liz R, Medeiros YS, Fröde TS: Efficacy of tacrolimus in inhibiting inflammation caused by carrageenan in a murine model of air pouch. Transpl Immunol 2008, 19:25–29
43. Pereira R, Medeiros YS, Fröde TS: Antiinflammatory effects of tacrolimus in a mouse model of pleurisy. Transpl Immunol 2006, 16:105–111

JOURNAL OF CLINICAL MICROBIOLOGY, Dec. 2009, p. 4141–4143 Vol. 47, No. 12
0095-1137/09/$12.00 doi:10.1128/JCM.01437-09
Copyright © 2009, American Society for Microbiology. All Rights Reserved.

Evaluation of Hepatitis C Virus Core Antigen Assays in Detecting Recombinant Viral Antigens of Various Genotypes[▽]

Mohsan Saeed,[1,3] Ryosuke Suzuki,[1] Madoka Kondo,[1] Hideki Aizaki,[1] Takanobu Kato,[1] Toshiaki Mizuochi,[2] Takaji Wakita,[1] Haruo Watanabe,[1,3] and Tetsuro Suzuki[1]*

Department of Virology II[1] and Department of Safety Research on Blood and Biological Products,[2] National Institute of Infectious Diseases, Tokyo 162-8640, and Department of Infection and Pathology, Graduate School of Medicine, The University of Tokyo, Hongo, Bunkyo-ku, Tokyo 113-0033,[3] Japan

Received 24 July 2009/Returned for modification 3 September 2009/Accepted 19 September 2009

A single substitution within the hepatitis C virus core antigen sequence, A48T, which is observed in ~30% of individuals infected with genotype 2a virus, reduces the sensitivity of a commonly used chemiluminescence enzyme immunoassay. Quantitation of the antigen is improved by using a distinct anticore antibody with a different epitope.

Hepatitis C virus (HCV) is a major cause of chronic liver disease throughout the world. Accurate diagnosis of HCV infection is important due to the morbidity associated with the virus, and determining the level of viral replication is important in predicting and monitoring the effect of antiviral treatment. Although quantifying viral RNA represents the standard method for identifying active infection (5, 8, 13), several sensitive immunoassays that detect the viral core antigen (Ag) have now been developed as an alternative to HCV RNA testing (3, 4, 6, 9, 10, 12, 16). The amino acid sequence of the core Ag is largely conserved among different viral isolates (14); however, genetic variability of the virus constitutes one of the major challenges to using core Ag assays for diagnosis. In this study, we examined the effects of sequence heterogeneity on the sensitivity of diagnostic kits for detection of the core Ag by using recombinant Ag derived from each of the major HCV genotypes. Expression plasmids for epitope-tagged core Ag were generated by inserting cDNA for the full-length core region of genotype 1a (17; GenBank accession no. AF011751), 1b (1; D89815), 2a (7; AB047639), 2b (AB030907), or 3a virus, with a FLAG tag sequence attached at its 5′ end, into the EcoRI site of the pCAG mammalian expression vector (11). HEK293T cells transiently transfected with the expression plasmids were harvested 48 h after transfection using a passive lysis buffer (Promega, Madison, WI). Centrifugation was performed to remove the debris after ultrasonication. Total protein was quantified in aliquots of cell lysate by using the bicinchoninic acid method (Pierce, Rockford, IL) and then used for determining the concentrations of HCV core Ag.

Figure 1A shows comparable levels of core Ag in each sample of cell lysate, as determined by immunoblotting with anti-FLAG antibody (Ab). The ability of HCV core Ag assays to detect five different HCV genotypes were compared using a commercially available chemiluminescence enzyme immunoassay (CLEIA) (Lumipulse II HCV core assay [assay detection range, approximately 50 to 50,000 fmol/liter]; Fujirebio, Japan) (15) and enzyme-linked immunosorbent assay (ELISA) (Ortho HCV Ag ELISA test [assay detection range, approximately 44.4 to 3,600 fmol/liter]; Ortho-Clinical Diagnostics, Japan) (2) to detect HCV core Ag in cell lysate. As shown in Fig. 1B,

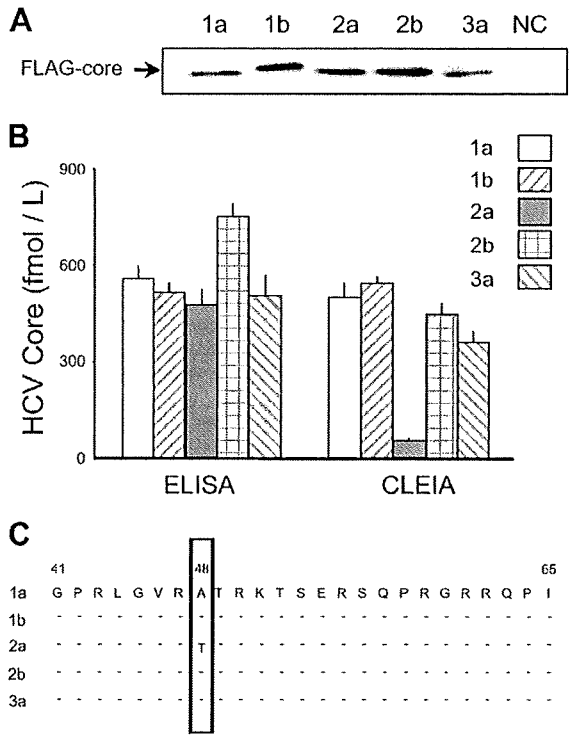

FIG. 1. Detection of recombinant HCV core Ag derived from genotype 1a, 1b, 2a, 2b, and 3a isolates by immunoblotting using an anti-FLAG Ab (A) as well as ELISA and CLEIA (B). The data shown in panel B represent the mean values and standard deviations (n = 3). NC, negative control. (C) The amino acid sequence from amino acids 41 to 65 of the core Ag used in this study. Key residues at the 48th position are boxed. Hyphens indicate conservation.

* Corresponding author. Mailing address: Department of Virology II, National Institute of Infectious Diseases, 1-23-1 Toyama, Shinjuku-ku, Tokyo 162-8640, Japan. Phone: 81-3-5285-1111. Fax: 81-3-5285-1161. E-mail: tesuzuki@nih.go.jp.

[▽] Published ahead of print on 7 October 2009.

Downloaded from jcm.asm.org at National Institute of Infectious Diseases on December 2, 2009

TABLE 1. Comparison of the 48th residues of HCV core Ags of genotypes 1a, 1b, 2a, 2b, and 3a

Genotype	No. of isolates	No. (%) of isolates with residue at 48th position		
		T	A	Other
1a	263	9 (3.5)	254 (96.5)	0 (0)
1b	298	2 (0.7)	294 (98.6)	2 (0.7)
2a	17	5 (29.5)	12 (70.5)	0 (0)
2b	17	0 (0)	17 (100)	0 (0)
3a	23	0 (0)	23 (100)	0 (0)
Total	618	16 (2.6)	600 (97.1)	2 (0.3)

although the ELISA measured similar concentrations of core Ag in all samples, apparent low levels of the genotype 2a core Ag, originally from an isolate known as the JFH-1 isolate (7), were detected using the CLEIA method, suggesting that some differences in the amino acid sequences corresponding to particular HCV genotypes or isolates may influence the sensitivity of core Ag detection. A comparison of the core Ag sequences, including the monoclonal Ab epitopes used in the development of CLEIA, revealed conservation of alanine at the 48th position in four clones, of genotypes 1a, 1b, 2b, and 3a, but not genotype 2a, for which there is a threonine at this position (Fig. 1C). Based on our analysis of sequences available from the HCV database (http://hcv.lanl.gov/content/sequence/NEWALIGN/align.html), alanine is highly conserved at the 48th residue of the core Ag for HCV isolates of genotypes 1a, 1b, 2b, and 3a (Table 1). In contrast, alanine and threonine occur in this position in 70.5% and 29.5%, respectively, of genotype 2a isolates. To examine whether the low sensitivity of the CLEIA method might be due to this particular amino acid change, we next replaced threonine with alanine at the 48th position of the JFH-1 core Ag (for

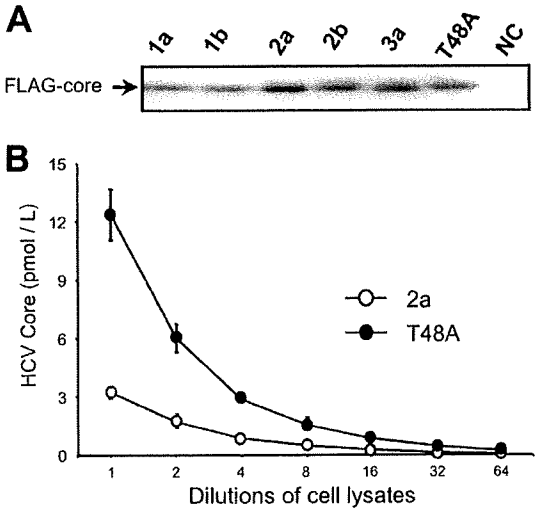

FIG. 2. Effect of T48A substitution in the core Ag of the JFH-1 isolate with regard to sensitivity of the CLEIA method. Samples of wild-type or mutated core Ag cell lysate were analyzed by immunoblotting (A) and CLEIA (B). The data shown in panel B represent the mean values and standard deviations (n = 3). NC, negative control.

TABLE 2. Comparison of the modified CLEIA with the original version for detection of the core Ags of genotypes 1a, 1b, 2a, 2b, and 3a[a]

Genotype	CLEIA	HCV core antigen concn (fmol/liter) in serially diluted cell lysates at indicated fold dilution							
		1	2	4	8	16	32	64	128
1a	Original	11,147	5,527	2,611	1,484	691	403	195	101
	Modified	10,511	5,700	2,676	1,420	716	444	200	111
1b	Original	11,612	5,618	3,081	1,551	779	409	223	113
	Modified	11,192	6,028	2,824	1,522	804	431	197	101
2a	Original	3,216	1,710	844	480	232	104	48	36
	Modified	12,101	6,255	3,153	1,676	805	422	212	106
2b	Original	10,559	5,635	2,811	1,286	762	387	194	94
	Modified	10,977	6,179	3,381	1,624	842	437	219	129
3a	Original	11,478	5,891	2,922	1,414	756	422	212	112
	Modified	11,208	6,225	3,126	1,555	791	445	215	100

[a] Data represent the mean values in triplicate measurements.

Downloaded from jcm.asm.org at National Institute of Infectious Diseases on December 2, 2009

the mutant JFH-1coreT48A) and measured the HCV core Ag concentration in cells expressing both mutated and wild-type JFH-1 core Ag. After confirming comparable levels of FLAG-tagged core Ag in the cell lysate samples by immunoblotting (Fig. 2A), HCV core Ag was quantified in the samples by serial dilution via the CLEIA method. As shown in Fig. 2B, the core Ag concentrations of JFH-1coreT48A were assessed to be 3.2- to 3.8-fold higher than those of the wild-type core Ag, suggesting that the sensitivity of HCV core Ag detection may have been affected by the 48th residue in the core Ag. Data for samples derived from genotypes 1a, 1b, 2b, and 3a were analogous to data for JFH-1coreT48A (data not shown). Although HCV isolates with threonine at the 48th position of the core Ag sequence comprise a relatively small proportion of the major genotype population, only 2.6% of the genotype 1a, 1b, 2a, 2b, and 3a isolates here (16 of 618 isolates; Table 1), attempts to overcome this problem would improve the overall sensitivity and usefulness of the assay. To achieve this aim, another monoclonal anticore Ab, whose epitope is comprised of amino acids 50 to 65, which are completely conserved among all the genotypes examined (Fig. 1C), was therefore used as a second Ab in a modified version of the CLEIA. We compared this modified assay with the original version by measurement of core Ag concentrations of the various genotypes (Fig. 2A) as illustrated in Table 2. The modified assay was able to quantify core Ag from genotypes 1a, 1b, 2a, 2b, and 3a with no significant differences observed between Ag levels in samples from different genotypes at each dilution.

It has been demonstrated that the HCV core Ag assay is a useful alternative to HCV RNA quantification for the diagnosis of hepatitis C and for monitoring the antiviral effects of treatment. Compared to various reverse transcription-PCR methods, HCV core assays are less expensive and easier to perform, without the requirement of sophisticated laboratory equipment and specially trained laboratory personnel. In addition, the core Ag assay can be used to measure a more diverse set of blood samples, such as sera stored for a long period of time, because the viral Ag is generally more stable than the RNA in sera or plasma. Despite the adequate performance of core Ag assays, we have shown that a single amino acid substitution at the 48th position of the core Ag changes the detection sensitivity. It is also noted that, although the original CLEIA should be improved, the ELISA used in this study may be substituted for it.

In conclusion, we have identified a distinct anticore Ab with a different epitope that might enable improved detection across all of the major HCV isolates. The findings of this study would provide useful information for the development of an improved assay with greater accuracy.

We thank Ortho-Clinical Diagnostics K.K. and Fujirebio Inc. for providing the diagnostic kits and for helping us in performing the assays.

This work was supported by a grant-in-aid for scientific research from the Ministry of Health, Labor and Welfare of Japan.

REFERENCES

1. **Aizaki, H., Y. Aoki, T. Harada, K. Ishii, T. Suzuki, S. Nagamori, G. Toda, Y. Matsuura, and T. Miyamura.** 1998. Full-length complementary DNA of hepatitis C virus genome from an infectious blood sample. Hepatology **27:** 621–627.
2. **Aoyagi, K., C. Ohue, K. Iida, T. Kimura, E. Tanaka, K. Kiyosawa, and S. Yagi.** 1999. Development of a simple and highly sensitive enzyme immunoassay for hepatitis C virus core antigen. J. Clin. Microbiol. **37:**1802–1808.
3. **Bouvier-Alias, M., K. Patel, H. Dahari, S. Beaucourt, P. Larderie, L. Blatt, C. Hezode, G. Picchio, D. Dhumeaux, A. U. Neumann, J. G. McHutchison, and J. M. Pawlotsky.** 2002. Clinical utility of total HCV core antigen quantification: a new indirect marker of HCV replication. Hepatology **36:**211–218.
4. **Buti, M., C. Mendez, M. Schaper, S. Sauleda, A. Valdes, F. Rodriguez-Frias, R. Jardi, and R. Esteban.** 2004. Hepatitis C virus core antigen as a predictor of non-response in genotype 1 chronic hepatitis C patients treated with peginterferon alpha-2b plus ribavirin. J. Hepatol. **40:**527–532.
5. **Chevaliez, S., and J. M. Pawlotsky.** 2007. Practical use of hepatitis C virus kinetics monitoring in the treatment of chronic hepatitis C. J. Viral Hepat. **14** (Suppl. 1)**:**77–81.
6. **González, V., E. Padilla, M. Diago, M. D. Gimenez, R. Sola, L. Matas, S. Montoliu, R. M. Morillas, C. Perez, and R. Planas.** 2005. Clinical usefulness of total hepatitis C virus core antigen quantification to monitor the response to treatment with peginterferon alpha-2a plus ribavirin. J. Viral Hepat. **12:**481–487.
7. **Kato, T., A. Furusaka, M. Miyamoto, T. Date, K. Yasui, J. Hiramoto, K. Nagayama, T. Tanaka, and T. Wakita.** 2001. Sequence analysis of hepatitis C virus isolated from a fulminant hepatitis patient. J. Med. Virol. **64:**334–339.
8. **Laperche, S.** 2005. Blood safety and nucleic acid testing in Europe. Euro Surveill. **10:**3–4.
9. **Maynard, M., P. Pradat, P. Berthillon, G. Picchio, N. Voirin, M. Martinot, P. Marcellin, and C. Trepo.** 2003. Clinical relevance of total HCV core antigen testing for hepatitis C monitoring and for predicting patients' response to therapy. J. Viral Hepat. **10:**318–323.
10. **Netski, D. M., X. H. Wang, S. H. Mehta, K. Nelson, D. Celentano, S. Thongsawat, N. Maneekarn, V. Suriyanon, J. Jittiwutikorn, D. L. Thomas, and J. R. Ticehurst.** 2004. Hepatitis C virus (HCV) core antigen assay to detect ongoing HCV infection in Thai injection drug users. J. Clin. Microbiol. **42:**1631–1636.
11. **Niwa, H., K. Yamamura, and J. Miyazaki.** 1991. Efficient selection for high-expression transfectants with a novel eukaryotic vector. Gene **108:**193–199.
12. **Nübling, C. M., G. Unger, M. Chudy, S. Raia, and J. Lower.** 2002. Sensitivity of HCV core antigen and HCV RNA detection in the early infection phase. Transfusion **42:**1037–1045.
13. **Roth, W. K., M. Weber, and E. Seifried.** 1999. Feasibility and efficacy of routine PCR screening of blood donations for hepatitis C virus, hepatitis B virus, and HIV-1 in a blood-bank setting. Lancet **353:**359–363.
14. **Suzuki, T., K. Ishii, H. Aizaki, and T. Wakita.** 2007. Hepatitis C viral life cycle. Adv. Drug Deliv. Rev. **59:**1200–1212.
15. **Takahashi, M., H. Saito, M. Higashimoto, K. Atsukawa, and H. Ishii.** 2005. Benefit of hepatitis C virus core antigen assay in prediction of therapeutic response to interferon and ribavirin combination therapy. J. Clin. Microbiol. **43:**186–191.
16. **Tanaka, E., C. Ohue, K. Aoyagi, K. Yamaguchi, S. Yagi, K. Kiyosawa, and H. J. Alter.** 2000. Evaluation of a new enzyme immunoassay for hepatitis C virus (HCV) core antigen with clinical sensitivity approximating that of genomic amplification of HCV RNA. Hepatology **32:**388–393.
17. **Yanagi, M., R. H. Purcell, S. U. Emerson, and J. Bukh.** 1999. Hepatitis C virus: an infectious molecular clone of a second major genotype (2a) and lack of viability of intertypic 1a and 2a chimeras. Virology **262:**250–263.

Downloaded from jcm.asm.org at National Institute of Infectious Diseases on December 2, 2009

Antiviral Research 85 (2010) 520–524

Contents lists available at ScienceDirect

Antiviral Research

journal homepage: www.elsevier.com/locate/antiviral

Identification of hepatitis C virus genotype 2a replicon variants with reduced susceptibility to ribavirin

Su Su Hmwe[a,b], Hideki Aizaki[a], Tomoko Date[a], Kyoko Murakami[a], Koji Ishii[a], Tatsuo Miyamura[a], Kazuhiko Koike[b], Takaji Wakita[a], Tetsuro Suzuki[a,*]

[a] Department of Virology II, National Institute of Infectious Diseases, 1-23-1 Toyama, Shinjuku-ku, Tokyo 162-8640, Japan
[b] Department of Gastroenterology, Graduate School of Medicine, University of Tokyo, 7-3-1 Hongo, Bunkyo-ku, Tokyo 113-8655, Japan

ARTICLE INFO

Article history:
Received 8 April 2009
Received in revised form 19 October 2009
Accepted 18 December 2009

Keywords:
Hepatitis C virus
Replication
Ribavirin
Drug resistance

ABSTRACT

Ribavirin (RBV), a nucleoside analogue, is used in the treatment of hepatitis C virus (HCV) infection in combination with interferons. However, potential mechanisms of RBV resistance during HCV replication remain poorly understood. Serial passage of cells harboring HCV genotype 2a replicon in the presence of RBV resulted in the reduced susceptibility of the replicon to RBV. Transfection of fresh cells with RNA from RBV-resistant replicon cells demonstrated that the RBV resistance observed is largely replicon-derived. Four major amino acid substitutions: T1134S in NS3, P1969S in NS4B, V2405A in NS5A, and Y2471H in NS5B region, were identified. Site-directed mutagenesis of these mutations into the replicon indicated that Y2471H plays a role in the reduced susceptibility to RBV and leads to decrease in replication fitness. The results, in addition to analysis of sequence database, suggest that HCV variants with reduced susceptibility to RBV identified are preferential to genotype 2a.

© 2010 Elsevier B.V. All rights reserved.

1. Introduction

Hepatitis C virus (HCV) is a leading cause of chronic liver diseases, such as chronic hepatitis, cirrhosis and hepatocellular carcinoma, affecting approximately 170 million people worldwide (WHO, 2000). HCV belongs to the genus Hepacivirus of the family Flaviviridae, and its genome is a single-stranded, positive-sense RNA of 9.6 kb. HCV displays marked genetic heterogeneity and is currently classified into 6 major genotypes and more than 50 subtypes. HCV genotypes have regional distribution and, of those, genotypes 1 and 2 are detected worldwide (Simmonds et al., 2000). Current standard therapy for chronic hepatitis C consists of the combination of pegylated interferon alpha (IFN-α) in combination with ribavirin (RBV). However, approximately 50% of treated patients infected with genotype 1 do not respond or show only a partial or transient response and treatment is limited by the adverse effects of both agents (Manns et al., 2001; Fried et al., 2002).

HCV replication is associated with a high rate of mutation that gives rise to a mixed and changing population of mutants, known as quasispecies (Martell et al., 1992; Domingo, 1996). The characteristic of HCV may have important implications concerning viral persistence, pathogenicity and resistance to antiviral agents (Domingo, 1996; Forns et al., 1999; Farci and Purcell, 2000). Most previous studies on the possible relationship between HCV quasispecies and response to chemotherapy have been carried out in HCV genotype 1 patients. In addition, several studies have successfully demonstrated that the HCV subgenomic replicon is derived from genotype 1, which typically contains HCV nonstructural genes placed downstream of the neomycin phosphotransferase gene, in selecting variants resistant to antiviral inhibitors. Two studies have demonstrated the identification of HCV genotype 1 mutants responsible for decreased sensitivity to RBV (Young et al., 2003; Pfeiffer and Kirkegaard, 2005). However, little is known about the generation of genotype 2 isolates resistant to antivirals including RBV, or the molecular mechanisms that confer resistance.

In this study, we report the generation and characterization of HCV genotype 2a replicon variants with reduced susceptibility to RBV. The impacts of major amino acid substitutions observed on RBV susceptibility and viral replication capacity were also examined.

2. Materials and methods

2.1. Compounds

RBV and IFN-α were purchased from MP Biomedicals (Eschwege, Germany) and Dainippon Sumitomo Pharma (Osaka, Japan), respectively.

* Corresponding author. Tel.: +81 3 5285 1111; fax: +81 3 5285 1161.
E-mail address: tesuzuki@nih.go.jp (T. Suzuki).

0166-3542/$ – see front matter © 2010 Elsevier B.V. All rights reserved.
doi:10.1016/j.antiviral.2009.12.008

Table 1
Primers used for PCR and nucleotide sequencing.

Region	Primer name	Nucleotide sequence	Position[a]	Polarity
NS3-4A-4B region	PCR primers			
	JF1S	GAAAAACACGATGATACCATG	1756–1776	Sense
	JF1AS	AACCCAGTCCCACACGTC	4650–4633	Antisense
	Sequencing primers			
	JF5S	CACTTTCAGTGACAACAGCA	2322–2341	Sense
	JF6S	CGCCACCGACGCCCTCATGA	3003–3022	Sense
	JF4AS	CTGGTCGACAACGGACTGGT	4109–4090	Antisense
NS5A-NS5B region	PCR primers			
	JF2S	TGCTCCGGATCCTGGCTC	4612–4629	Sense
	JF2AS	TACCTAGTGTGTGCCGCTCTA	7786–7806	Antisense
	Sequencing primers			
	JF3S	TGAGGTCCATGCTAACAGA	5209–5228	Sense
	JF4S	TCGAGGGGGAGCCTGGAGAT	5870–5889	Sense
	JF3AS	GAGTGTCTAACTGTTTCCCAG	7220–7200	Antisense

[a] Reference strain: Gene Bank accession no. AB114136.

2.2. Cell culture

The human hepatoma cell line Huh-7 was maintained in Dulbecco's modified Eagle's medium (DMEM) supplemented with MEM non-essential amino acids (Invitrogen) 100 units/ml penicillin, 100 μg/ml streptomycin, and 10% fetal bovine serum (FBS) at 37 °C in a 5% CO_2 incubator. HCV replicon cells JFH-1/4-1 (Miyamoto et al., 2006), which are Huh-7-derived cells carrying a subgenomic replicon of JFH-1 (Kato et al., 2003) were maintained in the Huh-7 medium as above, supplemented with 1 mg/ml G418 (Nacalai Tesque, Kyoto, Japan).

2.3. Quantification of HCV RNA

Total RNA was isolated from harvested cells using Trizol (Invitrogen). Copy numbers of the viral RNA were determined by real-time RT-PCR involving single-tube reactions and performed using TaqMan EZ RT-PCR Core Reagents (PE Applied Biosystems, Foster City, CA, USA), as described previously (Aizaki et al., 2003; Takeuchi et al., 1999).

2.4. Cell viability assay

Cells were seeded at density of 5×10^4 cells/well in 24-well plates and RBV at various concentrations was added on the next day. Cultures were further incubated for 3 days at 37 °C under a humidified 5% CO_2 atmosphere. Cytotoxicity assay was performed by Cell Titer-GLO™ Luminescent Cell Viability Assay (Promega, Madison, WI, USA) according to the manufacturer's instructions. Luciferase activities were quantified with LUMAT LB 9501 (Berthold Technologies, Bad Wilbad, Germany).

2.5. Isolation and nucleotide sequencing of HCV nonstructural regions from replicon-containing cells

Total cellular RNA was isolated from replicon cells with or without RBV treatment as described above. cDNA synthesis was carried out by using Super ScriptTM III First-Strand Synthesis System for RT-PCR (Invitrogen) with primer JF1AS for NS34AB region and JF2AS for NS5AB region. Two cDNA fragments, corresponding to NS3–NS4B and NS5A–NS5B regions, were amplified by PCR using Takara EX Taq DNA polymerase (Takara BIO, Kyoto, Japan) and specific primers (Table 1; Date et al., 2004). PCR products were subcloned into pGEM-T vector (Promega) and inserts were sequenced using QIA prep® Spin Mini Prep kit (QIAGEN, Tokyo, Japan). Nucleotide sequences were analyzed with the 3100 Avant Genetic Analyzer (PE Applied Biosystems).

2.6. Plasmid constructions

pSGR-JFH1/luc, a subgenomic replicon construct with luciferase reporter derived from HCV genotype 2a JFH-1 isolate was reported previously (Miyamoto et al., 2006). Mutant replicons carrying T1134S, P1969S, V2405A, and Y2471H were created by PCR-based site-directed mutagenesis and cDNA fragments containing the above mutations were inserted into the corresponding sites of pSGR-JFH/luc. All plasmids were confirmed by sequencing the entire PCR-generated inserts. Each mutant is referred to by the original amino acid (one letter code) followed by the residue positions within the complete open reading frame of full-length JFH-1 and the substituted amino acid (one letter code).

2.7. RNA synthesis and transient replication assay

The transient replication assay method was described previously (Kato et al., 2005). Briefly, purified plasmids of pSGR-JFH1/Luc, -JFH1/Luc-T1134S, -JFH/Luc-P1969S, -JFH/Luc-V2405A and -JFH/Luc-Y2471H were linearized with XbaI and were treated with proteinase K and SDS, followed by phenol–chloroform extraction. RNA was synthesized with Ampliscribe™ T7 Transcription Kits (Epicentre BIO Technologies, Madison, WI, USA). Each transcribed RNA (5 μg) was electroporated into 2.5×10^6 of Huh7 cells pulsed at 290 mV, 975uFD with Gene pulser II apparatus (Bio-Rad Laboratories, Hercules, CA, USA). Transfected cells were resuspended in growth medium without selection antibiotics and were plated in 24-well plates at 6×10^4 cells per well. Cells were harvested at different time points post-transfection and were lysed in Passive Lysis Buffer (Promega). Luciferase activity in cells was determined using the Luciferase Assay System (Promega).

3. Results

3.1. Selection of replicon variants derived from genotype 2a with reduced susceptibility to RBV

It has been reported that RBV inhibits HCV RNA replication in Huh-7 cells bearing the viral subgenomic replicon RNAs with the EC_{50} (50% effective concentration) values of 15–225 μM (Zhou et al., 2003; Tanaka et al., 2004; Kato et al., 2005; aus dem Siepen et al., 2007). To select for RBV-associated replicon variants, cells bearing a genotype 2a HCV replicon were serially passed in the presence of 200 μM RBV as well as 1 mg/ml G418. After 20-week treatment, variant cells were then tested for RBV resistance. HCV RNA levels were determined after a 72-h incubation with various concentrations of RBV in the absence of G418, and about 5-fold-reduced susceptibility to RBV was observed in the variant replicon

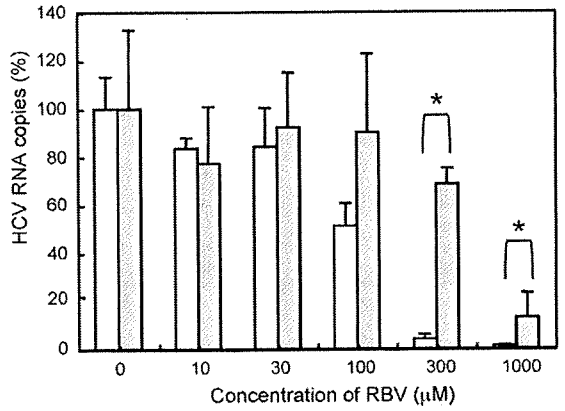

Fig. 1. Inhibitory effect of RBV on HCV RNA levels in genotype 2a replicon cells after long-term treatments with RBV. The replicon cells were serially passaged in 0 or 200 μM RBV for 20 weeks. The cells were then split and incubated with fresh RBV at various concentrations in the absence of G418 for 3 days, followed by the determination of HCV RNA. Clear bars, passage in the absence of RBV; gray bars, passage in the presence of RBV. HCV RNA copies per microgram of total RNA were normalized as percentages of those of untreated (RBV 0 μM). Each data point is presented as the mean of three independent determinations with standard deviation. $^*p < 0.05$.

cells; the EC_{50} values for the variant and wild-type replicon cells were 470 and 102 μM, respectively (Fig. 1). Comparable cytotoxic effects of RBV were observed against wild-type and variant replicon cells, with the CC_{50} (50% cytotoxicity concentration) values of 151 and 156 μM, respectively (data not shown).

3.2. Mapping RBV resistance to cell line or replicon RNA

To test whether reduced susceptibility to RBV in the variant cells observed as above was due to the appearance of mutations within the viral RNA or was cell-derived, total RNAs from the variant and wild-type replicon cells were extracted and used for retransfection of naïve Huh7 cells. Retransfected cells resistant to G418 were established after 4 weeks of cultures in the presence of 1 mg/ml G418 and were assessed for HCV RNA replication sensitivity to RBV (Fig. 2A). HCV RNA levels in the cells obtained from the wild-type replicon were inhibited by 56, 89 and 97% with 100, 300 and 1000 μM RBV, respectively. By contrast, the culture retransfected with RNA derived from the variant replicon cells exhibited inhibition levels of 13, 29 and 89% with the corresponding concentrations of RBV. EC_{50} values were calculated to be 93 and 449 μM, respectively. We confirmed the presence of replicon mutations, as described below, in the cells retransfected with RNA derived from the variant replicon cells.

In order to explore the possibility for cell-derived resistance, both wild-type and variant replicon cells were cured of viral RNAs by IFN treatment; cells were passaged with media containing 100 IU/mL IFN-α in the absence of G418 for 2 months. To compare RBV sensitivity, cured cells were transiently transfected with the wild-type JFH-1 subgenomic replicon RNA and were treated with various concentrations of RBV for 72 h. Similar anti-HCV effects of RBV were observed in the cured cells derived from wild-type and variant replicons, with the EC_{50} values of 147 and 118 μM, respectively (Fig. 2B). Thus, the results suggest that the RBV resistance observed may arise by mutations in the replicon rather than by changes in the cells.

3.3. HCV mutations in replicon variant with reduced susceptibility to RBV

It has been reported that mutations in RNA virus genomes responsible for RBV resistance are mostly present in the coding region for the viral RNA-dependent RNA polymerase (RdRp). On the other hand, it is known that RBV works as an RNA mutagen to generate rapidly mutating viral RNA and that NS5B RdRp and other nonstructural proteins in HCV are involved in the viral replication complex, playing key roles in genome replication. Therefore, we sequenced the coding regions for NS3 through NS5B proteins of the replicon molecules in order to determine whether mutations associated with RBV resistance were generated. As shown in Table 2, there were numerically more synonymous and non-synonymous mutations in the RBV-resistant variant replicon cells (RBV treatment) when compared with untreated replicative conditions (No-treatment) across most regions examined. Mutation frequencies of NS3, NS4B and NS5A regions of RBV treatment were significantly higher than those of No-treatment. The total number of synonymous mutations in the RBV-resistant variant replicon cells was 3 times higher than that under untreated replicative conditions, and the number of non-synonymous mutations in the RBV-resistant variant replicon cells was 1.5 times higher than that under untreated replicative conditions. The number of both synonymous and non-synonymous mutations (NS3, NS4B, NS5A and NS5B regions) in the RBV-resistant replicon cells was greater than that in the control cells. We also found a large number of transition

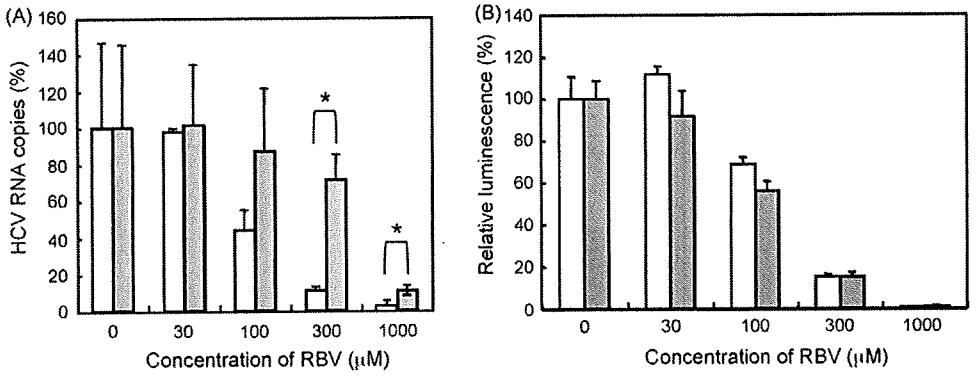

Fig. 2. Testing for replicon-derived resistance (A) or for cell-derived resistance (B). (A) Total RNA from RBV-resistant- or wild-type replicon cells was transfected into naïve Huh7 cells. After selection in 1 mg/ml G418 for 4 weeks, re-established replicon cells, wild-type derived (clear bars) and RBV resistance derived (gray bars), were treated with increasing concentrations of RBV in the absence of G418 for 3 days. HCV RNA copies per microgram total RNA were assessed and the levels from wild-type cells without RBV treatment were set at 100%. Data are indicated as means with standard deviations. $^*p < 0.05$. (B) RBV-resistant- or wild-type replicon cells were cured by passage in IFN-α in the absence of G418. Cured cells were transiently transfected with the replicon RNA derived from pSGR-JFH1/luc. Transient replication assay of transfectants derived from wild-type (clear bars) and RBV resistance (gray bars) was performed after treatment with various concentrations of RBV for 72 h. The values for wild-type-derived cells without RBV treatment were set at 100%. Data are indicated as means with standard deviations.

Table 2
Mutation frequencies in HCV NS regions after 20-weeks culture with or without RBV treatment.

Region	nt length	No-treatment			RBV treatment		
		No. of non-synonymous mutations[a]	No. of synonymous mutations[a]	Mutation frequency (10^{-3})	No. of non-synonymous mutations[a]	No. of synonymous mutations[a]	Mutation frequency (10^{-3})
NS3	1893	1.7 ± 2.1	2.3 ± 1.5	2.1	4.7 ± 2.4	6.5 ± 2.5	5.9[b]
NS4A	165	1.0 ± 1.0	0.3 ± 0.6	8.1	0.3 ± 0.5	0.5 ± 0.9	4.4
NS4B	780	1.3 ± 1.2	0.3 ± 0.6	2.1	2.3 ± 1.5	2.5 ± 1.2	4.7[c]
NS5A	1380	4.0 ± 1.2	2.0 ± 1.2	4.3	5.9 ± 1.2	6.2 ± 2.4	12.2[c]
NS5B	1773	4.5 ± 1.5	2.3 ± 1.5	3.8	4.8 ± 1.8	4.2 ± 1.1	9.0
NS3–NS5B	5991	12.5 ± 2.7	7.3 ± 2.7	-	17.8 ± 4.5	20.1 ± 4.6	-

[a] Values are means ± standard deviations.
[b] $p < 0.05$ relative to No-treatment by the unpaired t-test.
[c] $p < 0.01$ relative to No-treatment by the unpaired t-test.

mutations in RBV-resistant cells, particularly G-to-A and C-to-U transitions, as expected from previous studies. Although mutations were distributed throughout nonstructural regions, four major amino acid substitutions; T1134S in the NS3 region, P1969S in NS4B, V2405A in NS5A, and Y2471H in NS5B, not seen in wild-type cells were observed in most of the subclones among RBV-resistant replicon cells. T1134S, P1969S, V2405A, and Y2471H were present, respectively, in 7 of 11, 6 of 11, 8 of 13, and 7 of 13 PCR subclones sequenced.

3.4. Effects of T1134S, P1969S, V2405A, and Y2471H on RBV susceptibility

To test the possibility that any of the four mutations as identified confer resistance to RBV, we introduced these mutations individually into the JFH-1 subgenomic replicon containing a luciferase reporter gene. Cells transfected with mutant- or wild-type replicon RNA grown in the presence of various concentrations of RBV for 2 or 3 days. As demonstrated in Fig. 3A, the replication levels of all four mutant replicons (SGR-JFH1/Luc-T1134S, -P1969S, -V2405A, and -Y2471H) in the presence of 125 or 500 μM RBV were higher than those of the wild-type replicon. In particular, the Y2471H mutant significantly reduced susceptibility to RBV; replication levels of SGR-JFH1/Luc-Y2471H were 3–5-fold higher when compared to those of wild-type under the present assay conditions.

The relative replication activity of these mutant replicons was further determined in 3-day replication assay without drug treatment (Fig. 3B). All mutant replicons exhibited reduced efficiency relative to the wild-type replicon. Levels of the Y2471H-mutated replicon were approximately 30% of those of the wild-type, thus suggesting that replicon mutants with reduced sensitivity to RBV are associated with decreased replication fitness.

4. Discussion

It is generally accepted that, during chemotherapy against viral infection, high rates of viral replication and high frequencies of mutation lead to generation of drug-resistant mutants. Although several potential mechanisms for the inhibition of HCV replication by RBV have been proposed, the molecular mechanisms involved in the generation of RBV-resistant HCV remain poorly understood.

This study found that long-term treatment of HCV JFH-1-derived replicon cells with RBV leads to selection of preferential mutations in NS3 (T1134S), NS4B (P1969S), NS5A (V2405A) and NS5B (Y2471H) genes. Each mutation only required a single nucleotide change, and P1969S, V2405A and Y2471H are transition mutations, which are known to be commonly caused by incorporated RBV. Site-directed mutagenesis of these mutations into the replicon demonstrated that Y2471H plays a role in reduced susceptibility to RBV.

Crystal structure information revealed that HCV RdRp is organized into an arrangement with palm, fingers, and thumb subdomains (Lesburg et al., 1999). Residue 2471 (the 33rd position of NS5B) is present in the N-terminal loop region that bridges the fingers. Although this site is apparently distant from the active site of the polymerase in the palm region, it has been reported

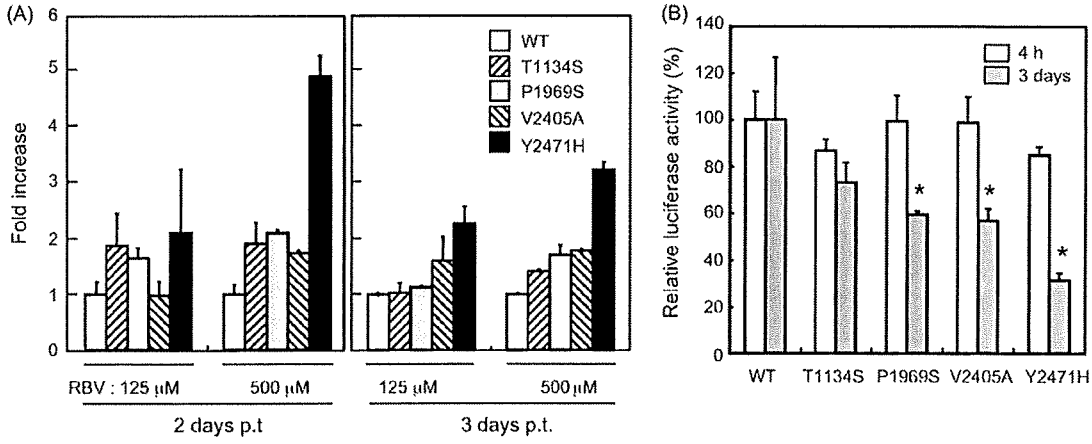

Fig. 3. Impact of major mutations in NS3–NS5B regions on RBV susceptibility (A) and replication capacity (B). Mutated replicons carrying single residue substitutions (T1134S, P1969S, V2405A, and Y2471H) were constructed and used for transient replication assay. Cells were transfected with either wild-type (WT) or with mutant replicon RNA in the absence or presence (125, 500 μM) of RBV. Luciferase activity was assessed at 4 h, 2 days and 3 days post-transfection (p.t.). (A) Luciferase activities of WT were set at 1, and the fold increases in the activities of mutants were plotted. (B) Luciferase activities in the absence of RBV at 4 h and 3 days post-transfection were shown. The activities of mutants were normalized as percentages of the WT activities. Data from triplicate samples were averaged and indicated with standard deviations. *$p < 0.05$ against WT.

that small molecules, such as benzimidazole compounds, are able to specifically bind the fingers-thumb interface and inhibit polymerase activity (Herlihy et al., 2008), thus suggesting that amino acid substitutions in the loop region may affect RNA polymerization. The involvement of tyrosine residue at position 415 of HCV NS5B in RBV resistance has been previously described for patients with genotype 1a infection and for the genotype 1b replicon (Young et al., 2003). Although the mechanism for resistance remains elusive, it has been hypothesized that RBV interacts with RdRp around this residue, which is located in the thumb subdomain, thus affecting RNA polymerization (Young et al., 2003).

Based on analysis of available sequences from Genbank, tyrosine at the 33rd residue of NS5B is conserved in all isolates of genotype 2a, but not in other genotypes. In genotype 1a and 1b isolates, 96% contain histidine and only a small population contains tyrosine or asparagine at the site. All the isolates of genotypes 3, 4, 5 and 6 contain histidine, whereas phenylalanine is conserved for genotype 2b. It should be noted that V2405 and P1969 are also completely conserved for genotype 2a but not for other genotypes. Therefore, it is likely that the identified HCV variants with reduced susceptibility to RBV are genotype-specific. It will be of interest to determine whether HCV genotype 2a is intrinsically more sensitive to RBV when compared with other genotypes.

At present, at least 4 mechanisms of action of RBV are proposed (Lau et al., 2002). They include (1) direct inhibition of the HCV replication machinery, (2) as an RNA mutagen that drives a rapidly mutating RNA virus over the threshold to "error catastrophe", (3) inhibition of the host enzyme inosine monophosphate dehydrogenase (IMPDH), and (4) enhancement of host T-cell-mediated immunity against viral infection. In addition to the direct inhibition, it is also possible that other mechanisms such as error-prone and IMPDH-inhibition are involved in HCV escape from RBV treatment. Further investigation of the interaction of HCV variants with the viral and cellular factors involved in viral resistance may improve understanding of the mechanism(s) of RBV resistance.

In conclusion, RBV encountered resistance from the HCV genotype 2a replicon largely mediated by mutations in the N-terminal region of NS5B. Although whether these mutagenic effects are also demonstrable in IFN-RBV combination therapy will require further studies, the mutations identified in this study represent the first drug-resistant variants belonging to HCV genotype 2a. The drug resistance patterns found in this study may be of benefit in prediction in vivo resistance profiles and the development of next-generation nucleoside analogues as anti-HCV drugs.

Acknowledgments

We thank M. Matsuda, S. Yoshizaki, M. Ikeda, T. Shimoji, M. Kaga and M. Sasaki for their technical assistance. This work was supported by a grant-in-aid for Scientific Research from the Japan Society for the Promotion of Science, from the Ministry of Health, Labour and Welfare of Japan and from the Ministry of Education, Culture, Sports, Science and Technology, and by Research on Health Sciences focusing on Drug Innovation from the Japan Health Sciences Foundation, Japan and by the Program for Promotion of Fundamental Studies in Health Sciences of the National Institute of Biomedical Innovation of Japan. S.S.H. is the recipient of a Research Resident Fellowship from Viral Hepatitis Research Foundation of Japan.

References

Aizaki, H., Nagamori, S., Matsuda, M., Kawakami, H., Hashimoto, O., Ishiko, H., Kawada, M., Matsuura, T., Hasumura, S., Matsuura, Y., Suzuki, T., Miyamura, T., 2003. Production and release of infectious hepatitis C Virus for human liver cell cultures in the three-dimensional radial-flow bioreactor. Virology 314, 16–25.

aus dem Siepen, M., Oniangue-Ndza, C., Wiese, M., Ross, S., Roggendorf, M., Viazov, S., 2007. Interferon-alpha and ribavirin resistance of Huh7 cells transfected with HCV subgenomic replicon. Virus Res. 125, 109–113.

Date, T., Kato, T., Miyamoto, M., Zhao, Z., Yasui, K., Mizokami, M., Wakita, T., 2004. Genotype 2a hepatitis C virus subgenomic replicon can replicate in HepG2 and IMY-N9 cells. J. Biol. Chem. 279, 22371–22376.

Domingo, E., 1996. Biological significance of viral quasispecies. Viral Hep. Rev. 2, 247–261.

Farci, P., Purcell, R.H., 2000. Clinical significance of hepatitis C virus genotypes and quasispecies. Semin. Liver Dis. 20, 103–126.

Forns, X., Purcell, R.H., Bukh, J., 1999. Quasispecies in viral persistence and pathogenesis of hepatitis C virus. Trends Microbiol. 7, 402–410.

Fried, T.R., Bradley, E.H., Towle, V.R., Allore, H., 2002. Understanding the treatment preferences of seriously ill patients. N. Engl. J. Med. 346, 1061–1066.

Herlihy, K.J., Graham, J.P., Kumpf, R., Patick, A.K., Duggal, R., Shi, S.T., 2008. Development of intragenotypic chimeric replicons to determine the broad-spectrum antiviral activities of hepatitis C virus polymerase inhibitors. Antimicrob. Agents Chemother. 52, 3523–3531.

Kato, T., Date, T., Miyamoto, M., Furusaka, A., Tokushige, K., Mizokami, M., Wakita, T., 2003. Efficient replication of the genotype 2a hepatitis C virus subgenomic replicon. Gastroenterology 125, 1808–1817.

Kato, T., Date, T., Miyamoto, M., Sugiyama, M., Tanaka, Y., Orito, E., Ohno, T., Sugihara, K., Hasegawa, I., Fujiwara, K., Ito, K., Ozasa, A., Mizokami, M., Wakita, T., 2005. Detection of anti-hepatitis C virus effects of interferon and ribavirin by a sensitive replicon system. J. Clin. Microbiol. 43, 5679–5684.

Lau, J.Y., Tam, R.C., Liang, T.J., Hong, Z., 2002. Mechanism of action of ribavirin in the combination treatment of chronic HCV infection. Hepatology 35, 1002–1009.

Lesburg, C.A., Cable, M.B., Ferrari, E., Hong, Z., Mannarino, A.F., Weber, P.C., 1999. Crystal structure of the RNA-dependent RNA polymerase from hepatitis C virus reveals a fully encircled active site. Nat. Struct. Biol. 6, 937–943.

Manns, M.P., McHutchison, J.G., Gordon, S.C., Rustgi, V.K., Shiffman, M., Reindollar, R., Goodman, Z.D., Koury, K., Ling, M., Albrecht, J.K., 2001. Peginterferon alfa-2b plus ribavirin compared with interferon alfa-2b plus ribavirin for initial treatment of chronic hepatitis C: a randomised trial. Lancet 358, 958–965.

Martell, M., Esteban, J.I., Quer, J., Genesca, J., Weiner, A., Esteban, R., Guardia, J., Gomez, J., 1992. Hepatitis C virus (HCV) circulates as a population of different but closely related genomes: quasispecies nature of HCV genome distribution. J. Virol. 66, 3225–3229.

Miyamoto, M., Kato, T., Date, T., Mizokami, M., Wakita, T., 2006. Comparison between subgenomic replicons of hepatitis C virus genotypes 2a (JFH-1) and 1b (con1 NK5.1). Intervirology 49, 37–43.

Pfeiffer, J.K., Kirkegaard, K., 2005. RBV resistance in hepatitis C virus replication containing cells conferred by changes in the cell line or mutations in the replicon RNA. J. Virol. 79, 2346–2355.

Simmonds, P., Gallin, J.I., Farrei, A.S., 2000. Hepatitis C virus genotypes. Biomed. Res. Rep. 2, 53–70.

Takeuchi, T., Katsume, A., Tanaka, T., Abe, A., Inoue, K., Tsukiyama Kohara, K., Kawaguchi, R., Tanaka, S., Kohara, M., 1999. Real-time detection system for quantification of Hepatitis C virus genome. Gastroenterology 116, 636–642.

Tanaka, Y., Sakamoto, N., Enomoto, N., Kurosaki, M., Ueda, E., Maekawa, S., Yamashiro, T., Nakagawa, M., Chen, C.-H., Kanazawa, N., Kakinuma, S., 2004. Synergistic inhibition of intracellular hepatitis C virus replication by combination of ribavirin and interferon-alpha. J. Infect. Dis. 189, 1129–1139.

World Health Organization (WHO), 2000. Hepatitis C: global prevalence (update). Weekly Epidemiological Record, WHO 75, 18–19.

Young, K.C., Lindsay, K.L., Lee, K.J., Liu, W.C., He, J.W., Milstein, S.L., Lai, M.M., 2003. Identification of a ribavirin-resistant NS5B mutation of hepatitis C virus during ribavirin monotherapy. Hepatology 38, 869–878.

Zhou, S., Liu, R., Baroudy, B.M., Malcolm, B.A., Reyes, G.R., 2003. The effect of ribavirin and IMPDH inhibitors on hepatitis C virus subgenomic replicon RNA. Virology 310, 333–342.

Anticancer Chemotherapy Inhibits MHC Class I–Related Chain A Ectodomain Shedding by Downregulating ADAM10 Expression in Hepatocellular Carcinoma

Keisuke Kohga, Tetsuo Takehara, Tomohide Tatsumi, Takuya Miyagi, Hisashi Ishida, Kazuyoshi Ohkawa, Tatsuya Kanto, Naoki Hiramatsu, and Norio Hayashi

Department of Gastroenterology and Hepatology, Osaka University Graduate School of Medicine, Osaka, Japan

Abstract

MHC class I–related chain A (MICA) is a ligand for the NKG2D-activating immunoreceptor that mediates activation of natural killer (NK) cells. The ectodomain of MICA is shed from tumor cells, which may be an important means of evading antitumor immunity. We previously reported that patients with hepatocellular carcinoma (HCC) display high levels of soluble MICA in circulation, which could be downregulated by chemotherapy. The present study shows that anti-HCC drugs suppress MICA ectodomain shedding by inhibiting expression of a disintegrin and metalloproteinase 10 (ADAM10). Both ADAM10 and CD44, a typical substrate of the ADAM10 protease, were expressed in human HCC tissues and HCC cells but not in normal liver tissues or cultured hepatocytes. Small interfering RNA–mediated knockdown experiments revealed that ADAM10 is a critical sheddase for both MICA and CD44 in HCC cells. Of interest is the finding that epirubicin clearly downregulated ADAM10 expression and MICA shedding in HCC cells; its suppressive effect on MICA shedding was abolished in ADAM10-depleted cells. Epirubicin treatment also enhanced the NKG2D-mediated NK sensitivity of HCC cells. Patients with HCC had significantly higher levels of serum-soluble CD44, which correlated well with serum-soluble MICA levels, thus suggesting a close link between ADAM10 activity and MICA shedding in these patients. Soluble MICA and CD44 levels were downregulated with a significant correlation in patients treated by transarterial chemoembolization using epirubicin. In conclusion, anticancer drugs can modulate expression of ADAM10, which is critically involved in MICA ectodomain shedding. Epirubicin therapy may have a previously unrecognized effect on antitumor immunity in HCC patients. [Cancer Res 2009;69(20):8050–7]

Introduction

Hepatocellular carcinoma (HCC) is one of the leading causes of cancer deaths worldwide. Chronic liver disease caused by hepatitis virus infection and nonalcoholic steatohepatitis leads to a predisposition for HCC, with liver cirrhosis, in particular, being considered a premalignant condition (1, 2). With regard to treatment, surgical resection or percutaneous techniques such as ethanol injection and radiofrequency ablation are considered to be choices for curable treatment of localized HCC, whereas transcatheter arterial chemoembolization (TACE) is a well-established technique for more advanced HCC (3). The liver contains a large compartment of innate immune cells [natural killer (NK) cells and natural killer T cells] and acquired immune cells (T cells; refs. 4, 5), but the activation of these immune cells after HCC treatments remains unclear. If such treatments can efficiently activate abundant immune cells in the liver, this could lead to the establishment of attractive new strategies for HCC treatment.

MHC class I–related chain A and B (MICA and MICB) are ligands for NKG2D expressed on a variety of immune cells (6). In contrast to classic MHC class I molecules, MICA/B are rarely expressed on normal cells but frequently on tumor cells (7–10). The engagement of MICA/B and NKG2D strongly activates NK cells and costimulates T cells, enhancing their cytolytic activity and cytokine production (11). Thus, the MICA/B-NKG2D pathway is an important mechanism by which the host immune system recognizes and kills transformed cells (12). In addition to those membrane-bound forms, MICA/B molecules are also cleaved proteolytically from tumor cells and appear as soluble forms in sera of patients with malignancy (13–15). Soluble MICA/B in circulation downregulates NKG2D expression and disturbs NKG2D-mediated antitumor immunity (9, 10, 13). We previously reported that soluble MICA could be detected in sera of HCC patients (16) and that TACE treatment reduces the levels of soluble MICA and thereby upregulates the expression of NKG2D (17). Thus, cancer therapy may have a beneficial effect on NKG2D-mediated immune responses.

The release of soluble MICA/B from tumor cells is impaired by metalloproteinase inhibitors, suggesting the involvement of members of the metzincin superfamily, such as ADAM proteins (14, 18). In addition, ERp5, related to protein disulfide isomerase, is required for the MICA shedding as it reduces disulfide bond of the α3 domain of MICA (19). Although it may not be a direct protease for MICA, it may enable proteolytic cleavage through conformational change. Recently, it was reported that MICA shedding of 293T fibroblast cells and HeLa cervical cancer cells was inhibited by silencing of the ADAM10 and ADAM17 proteases (20). This suggests that ADAM family proteins may be a therapeutic target for enhancing antitumor immunity, but how to therapeutically modulate these proteins is still not clear. Furthermore, it remains to be determined whether ADAMs can regulate MICA shedding in a clinical setting.

In the present study, we showed that ADAM10, but not ADAM17, was critically required for MICA shedding in human HCC cells. Of importance is the discovery that epirubicin, a widely used anti-HCC drug, was capable of downregulating ADAM10 expression and

---

Note: Supplementary data for this article are available at Cancer Research Online (http://cancerres.aacrjournals.org/).

K. Kohga, T. Takehara, and T. Tatsumi contributed equally to this work.

Requests for reprints: Norio Hayashi, Department of Gastroenterology and Hepatology, Osaka University Graduate School of Medicine, 2-2 Yamadaoka, Suita, Osaka 565-0871, Japan. Phone: 81-6-6879-3621; Fax: 81-6-6879-3629; E-mail: hayashin@gh.med.osaka-u.ac.jp.

©2009 American Association for Cancer Research.

doi:10.1158/0008-5472.CAN-09-0789

activity in HCC cells; it can thus inhibit MICA shedding and enhance NK sensitivity. ADAM10 was immunohistochemically detected in HCC tissues and a correlation was observed between soluble MICA levels and ADAM10 activity determined by soluble CD44 levels in HCC patients. The present study sheds light on previously unrecognized effects of an anticancer drug on modulating ADAM family proteins and MICA shedding and thus suggests a promising aspect for chemoimmunotherapy against human HCC.

Materials and Methods

Liver tissues and immunohistochemistry. Human HCC tissues (n = 8) and normal liver tissues (n = 2) obtained at surgical resection were used. Informed consent, under an institutional review board–approved protocol,

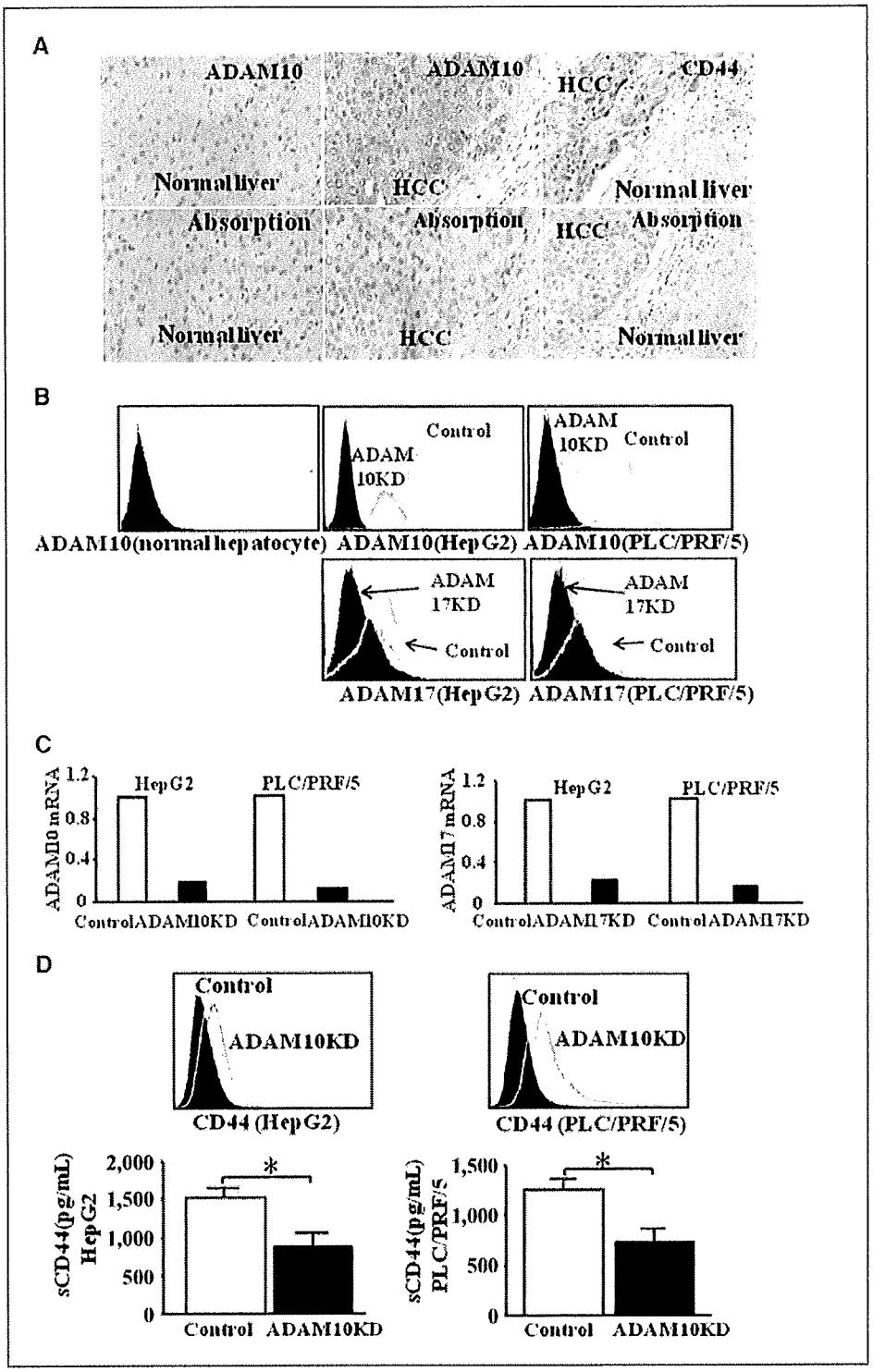

Figure 1. Expression of ADAM10 and CD44 in human HCC tissues and ADAM10 or ADAM17 knockdown in human HCC cells. *A*, immunohistochemical detection of ADAM10 and CD44 in human HCC tissues (n = 8) and normal liver tissues (n = 2). Liver sections were stained with the corresponding antibodies (*top panels*). Both primary antibodies were incubated with recombinant CD44 and ADAM10 proteins and then applied to liver sections in parallel as the absorption test (*bottom panels*). Representative images are shown. *B* and *C*, expression of ADAM10 or ADAM17 in human primary hepatocyte and HCC cell lines (*HepG2* and *PLC/PRF/5*). Cells were treated with ADAM10 siRNA, ADAM17 siRNA, or control siRNA, and subjected to analysis of ADAM10 or ADAM17 expression by flow cytometry (*B*) or real-time RT-PCR (*C*). *Histograms*, anti-ADAM10 or anti-ADAM17 staining of ADAM10 or ADAM17 siRNA-treated cells (*ADAM10KD* or *ADAM17KD, black dotted line*) and control siRNA-treated cells (*Control, gray line*), respectively. *Closed histograms*, control IgG staining. *D*, the expression of membrane-bound CD44 on HCC cells treated with ADAM10 siRNA (ADAM10KD, *black line*) or control siRNA (*Control, gray line*) was evaluated by flow cytometry (*top panels*). *Closed histograms*, control IgG staining. Soluble CD44 (*sCD44*) production from HCC cells treated with ADAM10 siRNA or control siRNA were evaluated by specific ELISA (*bottom panels*). *, $P < 0.05$.

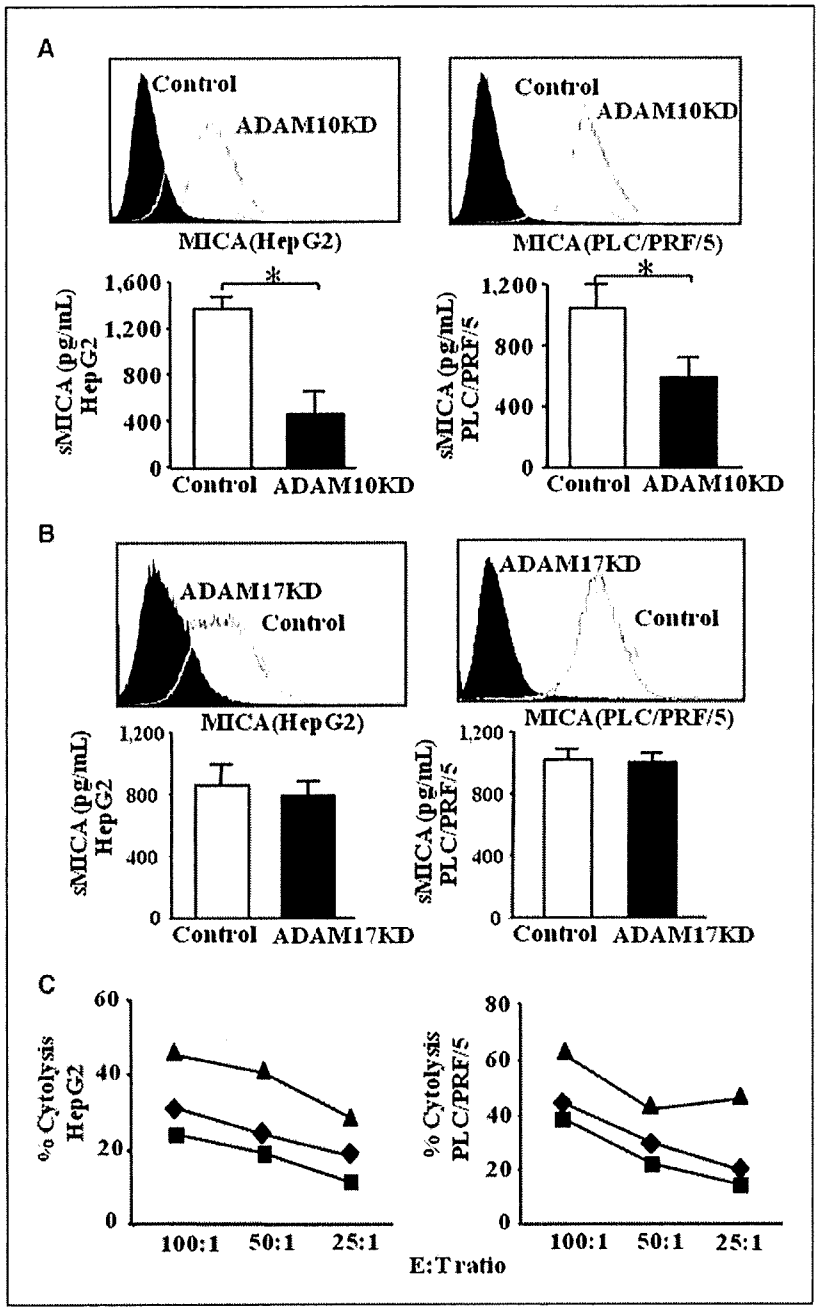

Figure 2. Expression of MICA in ADAM10 or ADAM17 knockdown HCC cells and NK sensitivity in ADAM10 knockdown HCC cells. *A* and *B*, the expression of membrane-bound MICA on HCC cells treated with ADAM10 siRNA (*ADAM10KD, black line*; *A*), ADAM17 siRNA (*ADAM17KD, black line*; *B*), or control siRNA (*Control, gray line*) was evaluated by flow cytometry (*top panels*). *Closed histograms*, control IgG staining. Soluble MICA (*sMICA*) production from HCC cells treated with ADAM10 siRNA (*A*), ADAM17 siRNA (*B*), or control siRNA were evaluated by specific ELISA (*bottom panels*). *, $P < 0.05$. *C*, HCC cells treated with ADAM10 siRNA or control siRNA were subjected to ^{51}Cr-release assay against NK cells. Cytolytic activity of NK cells against control HCC cells (■) or ADAM10 knockdown HCC cells without (▲) or with blocking antibody of MICA/B (6D4; ♦). Representative results are shown. Similar results were obtained from three independent experiments.

was obtained from all patients before sample acquisition. Liver sections were subjected to immunohistochemical staining using the ABC procedure (Vector Laboratories, Burlingame, CA). The primary antibodies used were anti-ADAM10 and anti-CD44 (R&D Systems). To confirm the specificity of the staining, primary antibodies were incubated with recombinant CD44 or ADAM10 protein (R&D Systems, Minneapolis, MN) for 3 h and then applied onto liver sections in parallel with staining of the primary antibodies as the absorption test.

HCC cell lines. Human HCC cell lines HepG2 and PLC/PRF/5 were purchased from the American Type Culture Collection and were cultured with DMEM supplemented with 10% fetal bovine serum (GIBCO/Life Technologies, Grand Island, NY) in a humidified incubator at 5% CO_2 and 37°C.

RNA silencing. The small interfering RNA (siRNA) method was used to knockdown ADAM10 and ADAM17. Stealth RNAi oligonucleotide targeting ADAM10 or ADAM17 and scrambled oligonucleotides as a control were purchased from Invitrogen (Carlsbad, CA). Cells were transfected by RNAi Max transfection reagent (Invitrogen) with 50 nmol/L siRNA. At 24 h posttransfection, the cells were analyzed for specific depletion of the mRNAs of ADAM10 and ADAM17 by real-time reverse transcription-PCR (RT-PCR; Applied Biosystems, Foster City, CA). The following siRNAs were used: ADAM10, 5′-AUAUCUGGGCAAUCACAG-CUUCUCG-3′; scramble control, 5′-AUACUUGGUCAACGCACUUCGAUGG-3′; ADAM17, 5′-UGAACAAGCUCUUCAGGUGGUUCUC-3′; scramble control, 5′-UGAUUAGAACUCUCGACUGGUGCUC-3′.

ELISA. The supernatants of cultured cells were harvested at 24 h after transfection with siRNA as well as sera from HCC patients (n = 97) and age-matched healthy volunteers (n = 32) were subjected to analysis of soluble MICA and soluble CD44 levels. Informed consent, under an institutional review board-approved protocol, was obtained from all patients before sample acquisition. The levels of soluble MICA and soluble CD44 were

determined by DuoSet MICA eELISA kit (R&D Systems) and soluble CD44std ELISA (Abcam, Cambridge, MA), respectively.

Flow cytometry. For the detection of membrane-bound MICA and CD44, cells were incubated with an anti-MICA–specific antibody (2C10, Santa Cruz Biotechnology, Santa Cruz, CA) or anti-CD44 antibody (R&D Systems) and stained with phycoerythrin (PE)-goat anti-mouse immunoglobulin (Beckman Coulter) as a secondary reagent and then subjected to flow cytometric analysis. For the detection of ADAM10 or ADAM17, cells were fixed and permeabilized with Cytofix/Cytoperm (BD Biosciences, San Jose, CA) and stained with PE-conjugated anti-ADAM10 or anti-ADAM17 antibody (R&D Systems). Flow cytometric analysis was performed using a FACScan flow cytometer (Becton Dickinson).

Plasmid construction of pMyc-MICA. MICA full coding cDNA was isolated from Huh7, human HCC cells, using a conventional RT-PCR method (Supplementary Fig. S1, DDBJ/EMBL/Genbank accession number AB506764) and inserted into the *Hin*dIII-*Xba*I site of pcDNA3 (Invitrogen). A C-myc tag was placed between the leader peptide and the α1 domain of MICA by site-specific mutagenesis using a QuikChange site-directed mutagenesis kit (Stratagene, La Jolla, CA) referred to as pMyc-MICA. Cells were transfected with pMyc-MICA using a Lipofectamine LTX reagent (Invitrogen). The green fluorescent protein (GFP)–expressing vector (pEGFP-C1, Clontech, Mountain View, CA) was cotransfected to evaluate the transfection efficiency.

Immunoprecipitation. Cells or tissues were homogenized in lysis buffer containing 1% NP40, 0.5% sodium deoxycholate, 0.1% SDS, 50 μg/mL aprotinin, 100 μg/mL phenylmethylsulfonyl fluoride, 1 mmol/L sodium orthovanadate, 50 mmol/L sodium fluoride, and PBS. To the cell supernatants, 0.5% NP40 and a cocktail of protease inhibitors were added. The protein contents of the samples were determined by BCA protein assay kit (Pierce, Rackford, IL). Immunoprecipitation with anti–c-Myc beads was performed for 1 h at 4°C. Immunocomplexes were eluted by a c-Myc–tagged peptide solution (MBL, Woburn, MA). The samples after immunoprecipitation were treated with 250 mU of N-glycosidase F (Roche, Mannheim, Germany) for 3 h at 37°C.

Western blotting. The total cellular protein was electrophoretically separated using SDS-12% polyacrylamide gels and transferred onto polyvinylidene difluoride membrane. The membrane was blocked in TBS-Tween containing 5% skim milk for 1 h and then probed with anti-Myc mouse monoclonal antibody (Cell Signaling Technology, Danvers, MA) at 4°C overnight. Horseradish peroxidase–conjugated anti-rabbit antibody and SuperSignal West Pico System (Pierce) were used for the detection of blots.

Real-time RT-PCR. Total RNA was isolated using RNeasy Mini Kit (Qiagen K.K., Tokyo, Japan) and was reverse transcribed using SuperScript III First-Strand Synthesis System (Invitrogen). The mRNA levels were evaluated using ABI PRISM 7900 Sequence Detection System (Applied Biosystems). Ready-to-use assays (Applied Biosystems) were used for the quantification of ADAM10 (Hs00153853_m1), ADAM17 (Hs00234221_m1), MICA (Hs00792195_m1), β-actin (Hs99999903_m1), and CD44 (Hs00174139_m1) mRNAs according to the manufacturer's instructions. The thermal cycling conditions for all genes were 2 min at 50°C and 10 min at 95°C, followed by 40 cycles at 95°C for 15 s and 60°C for 1 min. β-Actin mRNA from each sample was quantified as an endogenous control of internal RNA.

WST-8 assay. HepG2 and PLC/PRF/5 cells were treated with different concentrations of epirubicin for 24 h. Cell growth of epirubicin-treated HCC cells was determined by WST-8 assay (Nacalai Tesque, Kyoto, Japan) as previously described (21).

NK cell analysis. NK cells were isolated from human peripheral blood mononuclear cells by magnetic cell sorting using CD56 MicroBeads (Miltenyl Biotech, Auburn, CA) as previously described (16). The cytolytic ability of NK cells was assessed by 4-h ^{51}Cr-releasing assay with or without MICA/B-blocking antibody (6D4; ref. 7), which binds to the α1 and α2 domains of MICA and MICB. 6D4 was a generous gift from Drs. Veronika Groh and Thomas Spies (Fred Hutchinson Cancer Research Center, Seattle, WA).

Statistics. All values were expressed as the mean and SD. The statistical significance of differences between the groups was determined by applying Student's *t* test or two-sample *t* test with Welch correction after each group

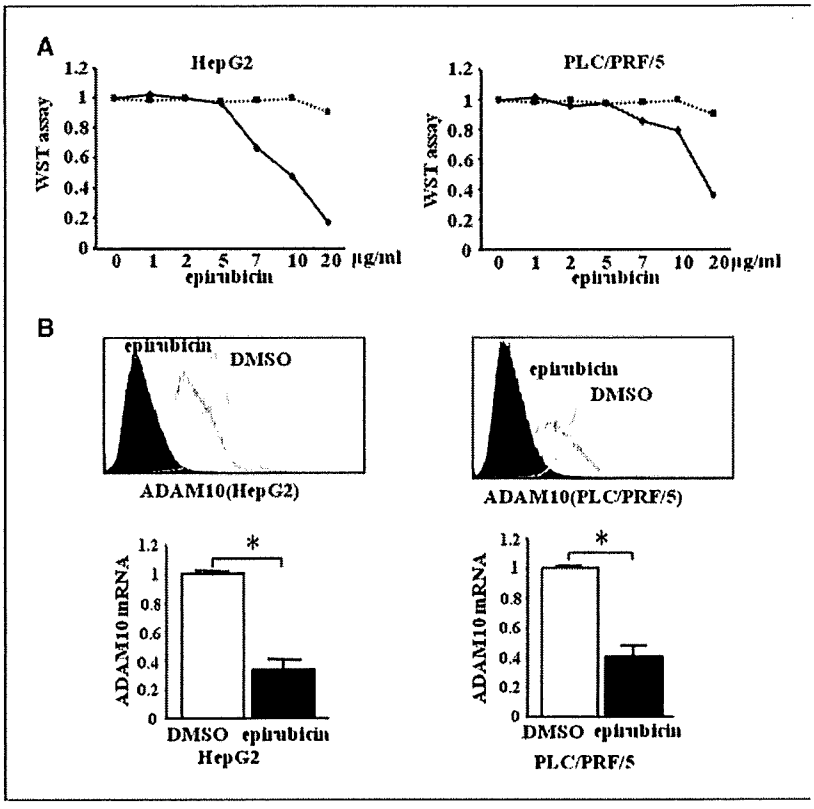

Figure 3. Expression of ADAM10 in epirubicin-treated HCC cells. *A*, the cytotoxicity of epirubicin to human HCC cells was evaluated by WST-8 assay. Cells were treated with different doses of epirubicin (*solid lines*) or vehicle (*DMSO*; *dotted lines*) for 24 h, and the viability of the cells was evaluated by the WST-8 assay. *B*, ADAM10 expression of epirubicin-treated HCC cells. Cells were treated with a nontoxic dose of 1 μg/mL epirubicin (*black lines*) or vehicle (DMSO, *gray lines*) for 24 h and their ADAM10 expression was evaluated by flow cytometry (*top panels*). *Closed histograms*, control IgG staining. Total RNA was extracted at 24 h of epirubicin treatment and mRNA levels of ADAM10 were evaluated by real-time RT-PCR (*bottom panels*). *, $P < 0.05$.

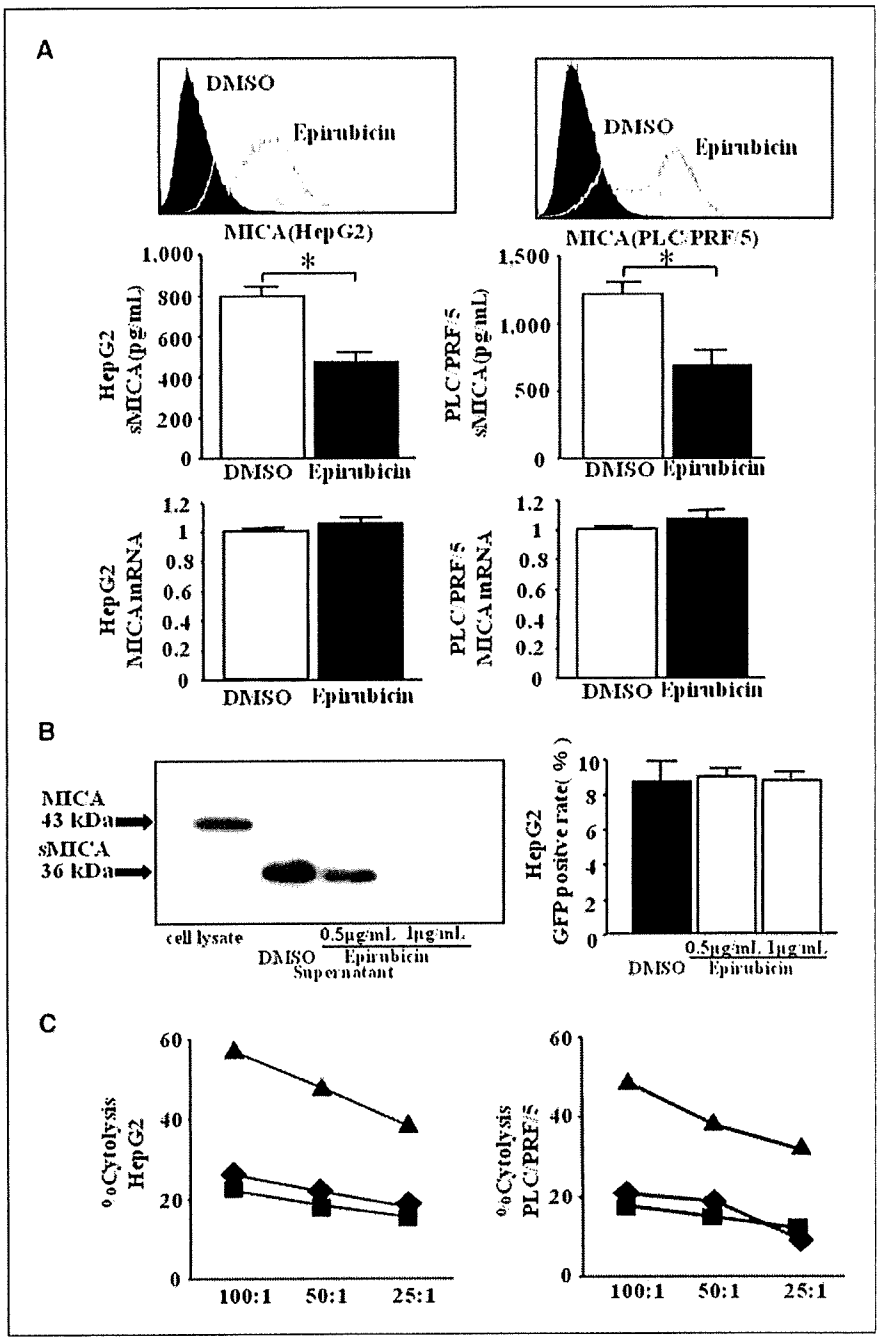

Figure 4. Expression and shedding of MICA in epirubicin-treated HCC cells. *A*, HCC cells were treated with a nontoxic dose of 1 μg/mL epirubicin (*black lines*) or vehicle (DMSO, *gray lines*) for 24 h and their expression of membrane-bound MICA and MICA mRNA was evaluated by flow cytometry (*top panels*) and real-time RT-PCR (*bottom panels*), respectively. *Closed histograms*, control IgG staining in flow cytometry. At the same time, 24-h culture supernatants were subjected to the analysis of soluble MICA (*sMICA*) levels by ELISA (*middle panels*). *, $P < 0.05$. *B*, HepG2 cells were transfected with pMyc-MICA and pEGFP-C1, cultured with 0.5 to 1 μg/mL epirubicin or vehicle (DMSO) for 24 h. Cell lysates from HepG2 cells and 24-h culture supernatants of epirubicin- or vehicle-treated HepG2 cells were immunoprecipitated with anti-Myc. The resulting immunoprecipitates were eluted, treated with N-glycanase, and subjected to Western blot analysis for MICA (*left*). Transfection efficacies were equal in all treatment groups as evidenced by similar GFP-positive cell rates (*right*). *C*, the cytolytic activity of NK cells against HCC cells. Vehicle-treated cells (■) or epirubicin-treated cells without (▲) or with blocking antibody of MICA/B (6D4; ♦) were subjected to ^{51}Cr-release assay. Representative results are shown. Similar results were obtained from three independent experiments.

had been tested with equal variance and Fisher's exact probability test. We defined statistical significance as $P < 0.05$.

Results

ADAM10 and CD44 are overexpressed in human HCC. ADAM10 was detected in all human HCC tissues tested by immunohistochemistry but not in normal liver tissues (Fig. 1*A*). Flow cytometric analysis revealed that ADAM10 was strongly expressed in a variety of HCC cell lines, including HepG2, PLC/PRF/5 (depicted in Fig. 1*B*), and Hep3B (data not shown), but faintly in primary hepatocytes. CD44, a typical substrate of the ADAM10 protease, was also expressed in all human HCC tissues but not in normal liver tissues (Fig. 1*A*). The data suggest that overexpression of ADAM10 and CD44 is a characteristic of human HCC like other malignancies (22).

ADAM10 is involved in MICA shedding of HCC cells but ADAM17 is not. To examine the involvement of ADAM family proteins in MICA ectodomain shedding, ADAM10 or ADAM17 were knocked down in HCC cells using a siRNA-mediated procedure. ADAM10 expression was clearly suppressed in HepG2 cells and PLC/PRF/5 cells at both mRNA and protein levels (Fig. 1*B* and *C*). Both cell lines expressed CD44 on the cellular surface and produced significant levels of soluble CD44 (Fig. 1*D*), indicating that CD44 is expressed and shed from those cell lines. ADAM10 knockdown (KD)

led to an increase in CD44 expression on HCC cells and a decrease in soluble CD44 levels in culture supernatants (Fig. 1*D*). Because ADAM10 has been established as being a sheddase for CD44, siRNA-mediated knockdown of ADAM10 suppressed not only the expression but also the activity of ADAM10 in HCC cells. HepG2 and PLC/PRF/5 cells also expressed ADAM17, which was clearly knocked down by a siRNA-mediated procedure (Fig. 1*B*).

HepG2 cells and PLC/PRF/5 cells expressed membrane-bound MICA and also produced soluble MICA (Fig. 2*A*). Knockdown of ADAM10 for both cell lines clearly upregulated MICA expression on their cellular surface and downregulated soluble MICA levels in their culture supernatant (Fig. 2*A*). In contrast, knockdown of ADAM17 did not affect the expression of membrane-bound MICA or the production of soluble MICA (Fig. 2*B*). We also examined the involvement of ADAM17 in MICA shedding of phorbol 12-myristate 13-acetate (PMA)–stimulated HCC cells because ADAM17 is considered to primarily affect stimulated shedding. The expression of membrane-bound MICA and the soluble MICA production were equal between PMA-stimulated ADAM17KD-HCC cells and control HCC cells (Supplementary Fig. S2). Thus, ADAM10, but not ADAM17, is critically involved in the shedding of MICA in HCC cells.

We next evaluated the cytolytic activity of NK cells against HCC cells. The cytolytic activity of NK cells against ADAM10KD-HepG2 cells was higher than that against control HepG2 cells. This activity was inhibited by blocking of anti-MICA/B antibody, suggesting that the increase of NK sensitivity depended on the increased expression of membrane-bound MICA on ADAM10KD-HepG2 cells, although we could not exclude the possibility of the involvement of MICB in this cytotoxicity (Fig. 2*C*). Similar results were also obtained with ADAM10KD-PLC/PRF/5 cells.

Epirubicin suppresses ADAM10 expression in HCC cells. We examined the biological modification of human HCC cells by adding epirubicin, which is commonly used in anti-HCC chemotherapy. We first examined the cytotoxicity of epirubicin to human HCC cells by WST-8 assay. Adding >5 μg/mL of epirubicin resulted in a significant decrease in cell growth of both HepG2 and PLC/PRF/5 cells (Fig. 3*B*). Based on these findings, we used 1 μg/mL of epirubicin to evaluate the biological effect on human HCC cells without toxicity. Both HepG2 cells and PLC/PRF/5 cells were cultured for 24 h with epirubicin and then subjected to analysis of ADAM10 expression. Epirubicin suppressed ADAM10 expression at the mRNA and protein levels in both cell lines (Fig. 3*C*). Although the data are not shown, doxorubicin also suppressed ADAM10 expression in HCC cells.

Epirubicin inhibits MICA ectodomain shedding and enhances susceptibility to NK cells of HCC cells. The above observations led us to investigate whether epirubicin or doxorubicin treatment would affect MICA ectodomain shedding in HCC cells. Epirubicin treatment led to an increase in membrane-bound MICA expression and a decrease in soluble MICA production in both HepG2 and PLC/PRF/5 cells (Fig. 4*A*). The mRNA levels of MICA did not change after exposure to epirubicin in both HCC cells (Fig. 4*A*). Similar data were obtained with doxorubicin-treated cells (data not shown).

To confirm whether the soluble MICA detected by ELISA was actually reflected in the cleaved form, we transfected Myc-tagged MICA into HepG2 cells and collected culture supernatants as well as cellular lysates. Immunprecipitates from these samples with anti-Myc were subjected to Western blot analysis after treatment with N-glycosidase. MICA in the culture supernatants migrated faster than cellular MICA (Fig. 4*B*), indicating that the MICA detected by ELISA is actually processed and released from full-length MICA. Epirubicin treatment led to a decrease in soluble MICA protein in HepG2 cells (Fig. 4*B*).

We next evaluated whether the epirubicin treatment could also modify the NK sensitivity of human HCC cells. Epirubicin-treated HepG2 cells or PLC/PRF/5 cells were more susceptible to NK cells than nontreated HepG2 or PLC/PRF/5 cells (Fig. 4*C*). The cytolytic activity against epirubicin-treated HCC cells was significantly decreased to the control levels by adding the anti-MICA/B blocking antibody. These results showed that the addition of epirubicin enhanced the NK sensitivity of HCC cell through increased

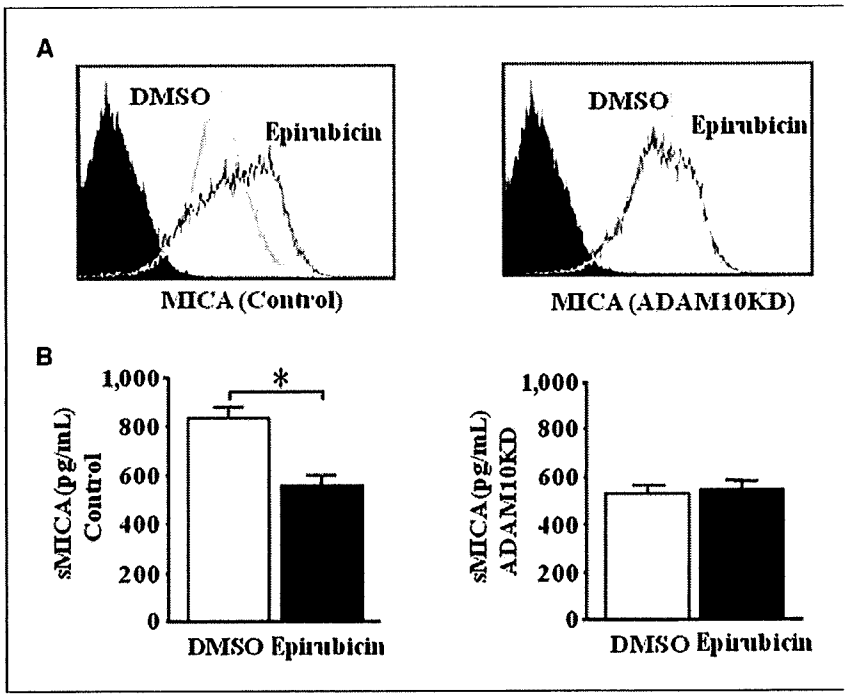

Figure 5. The epirubicin-mediated modification of MICA is ADAM10 dependent. HepG2 cells were transfected with ADAM10 siRNA (*ADAM10KD*) or control siRNA (*Control*) and further cultured with 1 μg/mL of epirubicin (*black lines*) or vehicle (DMSO, *gray line*) for 24 h. The expression of membrane-bound MICA (*MICA*) was evaluated by flow cytometry (*A*), and the soluble MICA (*sMICA*) production in the culture supernatant was evaluated by specific ELISA (*B*). Similar results were obtained from two independent experiments. *, $P < 0.05$.

expression of membrane-bound MICA, although the possibility of MICB involvement could not be excluded. The doxorubicin-treated human HCC cells showed similar results to those obtained from epirubicin-treated HCC cells (data not shown).

Epirubicin inhibits MICA ectodomain shedding through suppression of ADAM10. To examine whether the suppressive effect of epirubicin on MICA shedding occurred through downregulation of ADAM10, HepG2 cells were transfected with ADAM10 siRNA or scramble siRNA as a control and then treated with epirubicin. Consistent with earlier observations, epirubicin upregulated MICA surface expression and downregulated the levels of soluble MICA in control cells (Fig. 5). In contrast, neither upregulation of surface MICA nor downregulation of soluble MICA levels was observed in ADAM10KD-HepG2 cells. These results suggest that the suppressive effect of epirubicin on MICA shedding is mediated by ADAM10 downregulation. We also found similar results with ADAM10KD-PLC/PRF/5 cells (data not shown).

Soluble CD44 and soluble MICA levels in patients with HCC. We have shown that ADAM10 is expressed in human HCC tissues. However, it is not clear whether ADAM10 activity in HCC tissues is actually involved in MICA shedding in patients. Because ADAM10 was reported to be the constitutive functional sheddase of CD44 (23), we examined the soluble CD44 levels in HCC patients, which might be produced from tumor cells through ADAM10 activity. As shown in Fig. 6*A*, the soluble CD44 levels in HCC patients (n = 97) were significantly higher than those in age-matched healthy volunteers (n = 32). More importantly, soluble MICA levels in HCC patients significantly correlated with soluble CD44 levels (Fig. 6*B*), suggesting a close link between MICA shedding and ADAM10 activity.

We further examined soluble CD44 levels before and 2 weeks after TACE in HCC patients. Whereas the levels did not change in nontreated HCC patients during the 2-week interval (n = 9; 306.7 ± 82.5 ng/mL and 309.9 ± 79.9 ng/mL after 2 weeks), they were significantly decreased in epirubicin-based TACE-treated HCC patients (n = 21; 339.7 ± 78.1 ng/mL before TACE and 308.9 ± 81.4 ng/mL after TACE, $P < 0.003$). The changes of soluble CD44 in TACE treatment correlated significantly with those of soluble MICA (P = 0.0002; Fig. 6*C*). These results indicated that ADAM10-mediated CD44 shedding was decreased after TACE in HCC patients, implying that this reduction of ADAM10 activity might be related to the decline in MICA shedding.

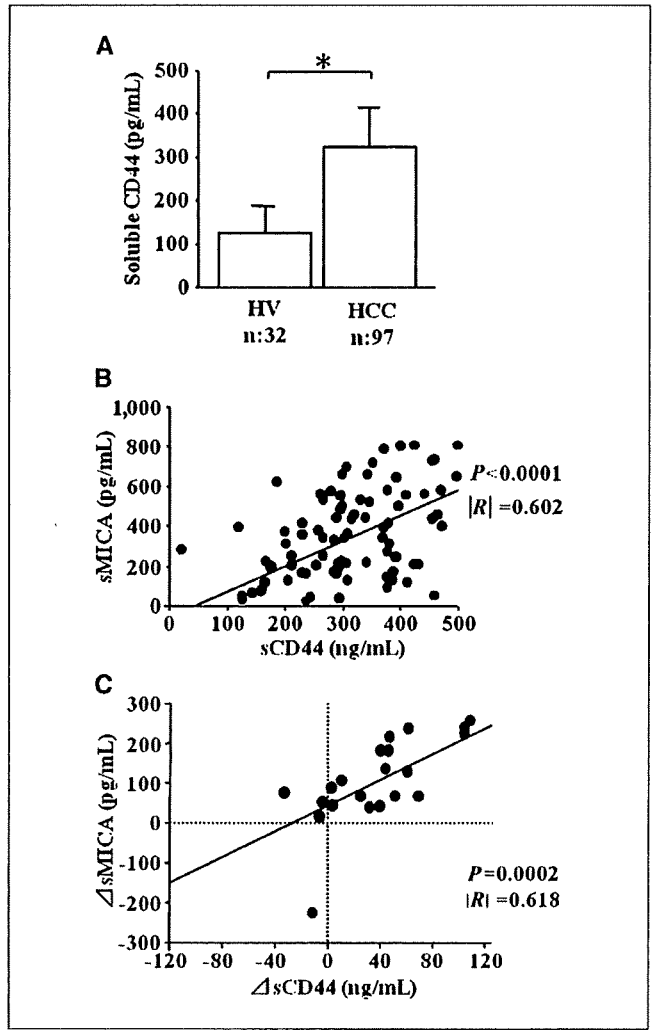

Figure 6. Correlation between soluble CD44 and soluble MICA in human HCC patients. *A* and *B*, soluble CD44 levels and MICA levels in healthy volunteers and HCC patients. Soluble CD44 levels (*sCD44*) and soluble MICA levels (*sMICA*) were determined for sera of HCC patients (n = 97) and age-matched healthy volunteers (*HV*; n = 32). *A*, comparison of sCD44 levels between groups; *B*, correlation between sCD44 levels and sMICA levels in 97 HCC patients. *, $P < 0.05$. *C*, correlation of sCD44 levels and sMICA levels during TACE therapy. HCC patients (n = 21) treated with epirubicin-based TACE therapy were enrolled and examined for sMICA and sCD44 levels before and 2 wk after therapy. Changes in sMICA (ΔsMICA = serum level of sMICA before TACE treatment − serum level of sMICA after TACE treatment) and those in sCD44 levels (ΔsCD44 = serum level of sCD44 before TACE treatment − serum level of sCD44 after TACE treatment) are plotted.

Discussion

MICA shedding is thought to be a principal mechanism by which tumor cells escape from NKG2D-mediated immunosurveillance (13). Thus, inhibition of MICA shedding should be a reasonable strategy for enhancing antitumor immunity. In the present study, we showed that ADAM10 was overexpressed in human HCC tissues and that ADAM10 knockdown resulted in increased expression of membrane-bound MICA, decreased production of soluble MICA, and upregulation of NK sensitivity of human HCC cells. These results point to ADAM10 as a therapeutic target for inhibiting MICA shedding, thereby ameliorating immunity against HCC. Waldhauer and colleagues recently showed that both ADAM10 and ADAM17 proteases are critically involved in the proteolytic release of soluble MICA of human 293T fibroblast cells and HeLa cervix carcinoma cells (20). Interestingly, in the present study, ADAM17 knockdown failed to affect MICA expression in human HepG2 cells or PLC/PRF/5 cells. Thus, ADAM10, not ADAM17, plays an essential role in the shedding of MICA in human HCC cells. Anderegg and colleagues (23) reported that only ADAM10, not ADAM17, contributed to shedding of CD44 molecules in human melanoma cells although both ADAM10 and ADAM17 proteases were significantly expressed in human melanoma tissues, suggesting that ADAM10 and ADAM17 do not always work in a similar manner. A recent report showed that ADAM10, but not ADAM17, could directly bind to calmodulin (24), which may involve the difference of MICA cleavage between ADAM10 and ADAM17 proteases. Recently, Boutet and colleagues reported that ADAM17 regulates proteolytic shedding of the MICB protein, which is another ligand for the NKG2D receptor on immune cells (25). We previously showed that both soluble MICA and MICB significantly increased in the sera of HCC patients and that therapeutic intervention for HCC leads to reduction of soluble

MICA levels, but not of soluble MICB levels (17), suggesting a more important role of soluble MICA in regulating NKG2D expression after HCC therapy. This led us to focus on the mechanism of MICA shedding in the present study.

Our results revealed that anticancer drugs such as epirubicin and doxorubicin downregulated ADAM10 expression and activity, thereby inhibiting MICA ectodomain shedding. The ADAM family proteins, which are highly expressed in some tumors, play a role in secreting growth factors, such as HB-EGF, and migration of cells. Thus, it is speculated that these proteins could be potential targets for tumor treatment (22). The present study is the first to show that clinically available anticancer drugs have an ability to modulate the expression of ADAM family proteins. They seem to suppress ADAM10 expression at a transcriptional level, but the precise mechanism of this suppression is not yet known.

The MICA ELISA system may not equally detect all soluble MICA (MICA molecules have >60 allelic variants). Our finding that soluble MICA could be detected in all HCC patients suggests that this system was applicable for our cohort of HCC patients. However, special caution should be paid for the use of this ELISA system for widely polymorphic MICA. Because CD44 is well known to be released into circulation from tumors by proteolytic cleavage of ADAM10 (23), the activity of ADAM10 in HCC tissues may be correlated with soluble CD44 levels. If so, our data suggest a close link between ADAM10 activity and the shedding of MICA in HCC. Furthermore, the decline in soluble MICA levels correlated well with the decline in soluble CD44 levels as early as 2 weeks after epirubicin-based TACE therapy. Reducing the tumor volume by such therapy may have led to both decreases but it is also possible that epirubicin suppresses ADAM10 activity, thereby inhibiting the shedding of MICA and CD44. Epirubicin may have a previously unrecognized role in cancer therapy; that is, affecting ADAM10 activity and MICA shedding rather than simply serving as a direct toxic agent for tumor cells.

Our data suggest that anti-HCC chemotherapy could remodel HCC cells, enhancing sensitivity to NK cells by upregulating MICA expression on the cellular surface. A concomitant decline in soluble MICA levels ameliorates NK cell ability by upregulating its NKG2D expression. We previously showed that activation of local innate antitumor immunity in liver tissues resulted in eliciting tumor-specific acquired immunity (21). If liver innate immunity is efficiently activated after anti-HCC chemotherapy, an additional antitumor effect against HCC cells could be expected. Immune modulators such as α-galactosylceramide have been shown to efficiently activate liver innate immune cells, including NK cells (21, 26). The combination therapy of anti-HCC chemotherapy and immunotherapy targeting NK cells might improve the antitumor effect of unresectable HCC and the prognosis of HCC patients.

In spite of recent progress in HCC therapies, there remains significant room for improvement, especially with respect to advanced liver cancer. We have shown here that anti-HCC chemotherapy resulted in enhanced NK sensitivity of HCC cells through inhibition of the activity of ADAM10 protease followed by modification of MICA expression. These findings indicate that efficient activation of liver innate immunity after anti-HCC chemotherapy might represent a particularly promising approach to suppress tumor growth and promote regression in liver cancer patients.

Disclosure of Potential Conflicts of Interest

No potential conflicts of interest were disclosed.

Acknowledgments

Received 3/4/09; revised 7/15/09; accepted 7/24/09; published OnlineFirst 10/13/09.

Grant support: Grant-in-Aid from the Ministry of Education, Culture, Sports, Science and Technology of Japan (T. Takehara) and Grant-in-Aid for Research on Hepatitis and BSE from the Ministry of Health, Labour and Welfare of Japan (N. Hayashi).

The costs of publication of this article were defrayed in part by the payment of page charges. This article must therefore be hereby marked *advertisement* in accordance with 18 U.S.C. Section 1734 solely to indicate this fact.

References

1. Fattovich G, Stroffolini T, Zagni I, Donato F. Hepatocellular carcinoma in cirrhosis: incidence and trends. Gastroenterology 2004;127:S35–50.
2. Bosch FX, Ribes J, Diaz M, Cleries R. Primary liver cancer: worldwide incidence and trends. Gastroenterology 2004;127:S5–16.
3. Takayasu K, Arii S, Ikai I, et al. Prospective cohort study of transarterial chemoembolization for unresectable hepatocellular carcinoma in 8510 patients. Gastroenterol 2006;131:461–9.
4. Doherty DG, O'Farrelly C. Innate and adaptive lymphoid cells in human liver. Immunol Rev 2000;174:5–20.
5. Mehal WZ, Azzaroli F, Crispe IN. Immunology of the healthy liver: old questions and new insights. Gatsroenterology 2001;120:250–60.
6. Bauer S, Groh V, Wu J, et al. Activation of NK cells and T cells by NKG2D, a receptor for stress-inducible MICA. Science 1999;285:727–9.
7. Groh V, Rhinehart R, Seceist H, Bauer S, Grabstein KH, Spies T. Broad tumor-associated expression and recognition by tumor-derived γδT cells of MICA and MICB. Proc Natl Acad Sci U S A 1999;96:6879–84.
8. Jinushi M, Takehara T, Tatsumi T, et al. Expression of MICA and MICB in human hepatocellular carcinomas and their regulation by retinoic acids. Int J Cancer 2003;104:354–61.
9. Wu JD, Higgins LM, Steinle A, Cosman D, Haugk K, Plymate SR. Prevalent expression of the immunostimulatory MHC class I chain-related molecule is counteracted by shedding in prostate cancer. J Clin Invest 2004;114:560–8.
10. Raffaghello L, Prigione I, Airoldi I, et al. Downregulation and/or release of NKG2D ligands as an immune evasion strategy of human neuroblastoma. Neoplasia 2004;6:558–68.
11. Ogasawara K, Lanier LL. NKG2D in NK and T cell-mediated immunity. J Clin Immunol 2005;25:534–40.
12. Coudert JD, Held W. The role of the NKG2D receptor for tumor immunity. Semin Cancer Biol 2006;16:333–43.
13. Groh V, Wu J, Yee C, Spies T. Tumor-derived soluble MIC ligands impair expression of NKG2D and T cell activation. Nature 2002;419:734–8.
14. Salih HR, Rammensee HG, Steinle A. Downregulation of MICA on human tumors by proteolytic shedding. J Immunol 2002;169:4098–102.
15. Salih HR, Antropius H, Gieseke F, et al. Functional expression and release of ligands for activating immunoreceptor NKG2D in leukemia. Blood 2003;102:1389–96.
16. Jinushi M, Takehara T, Tatsumi T, et al. Impairment of natural killer cell and dendritic cell functions by soluble form of MHC class I-related chain A in advanced human hepatocellular carcinoma. J Hepatol 2005;43:1013–20.
17. Kohga K, Takehara T, Tatsumi T, et al. Serum levels of soluble major histocompatibility complex (MHC) class I-related chain A in patients with chronic liver disease and changes during transcatheter arterial embolization for hepatocellular carcinoma. Cancer Sci 2008;99:1643–9.
18. Holdenrieder S, Stieber P, Peterfi A, Nagel D, Steinle A, Salih HR. Soluble MICA in malignant disease. Int J Cancer 2006;118:684–7.
19. Kaiser BK, Yim D, Chow IT, et al. Disulphide-isomerase-enabled shedding of tumor-associated NKG2D ligands. Nature 2007;447:482–6.
20. Waldhauer I, Goehlsdorf D, Gieseke F, et al. Tumor-associated MICA is shed by ADAM proteases. Cancer Res 2008;68:6368–76.
21. Tatsumi T, Takehara T, Yamaguchi S, et al. Intrahepatic delivery of α-galactosylceramide-pulsed dendritic cells suppresses liver tumor. Hepatology 2007;45:22–30.
22. Mochizuki S, Okada Y. ADAMs in cancer cell proliferation and progression. Cancer Sci 2007;98:161–7.
23. Anderegg U, Eichenberg T, Parthaune T, et al. Simon JC. ADAM10 is the constitutive functional sheddase of CD44 in human melanoma cells. J Invest Dermatol 2009;129:1471–82.
24. Nagano O, Murakami D, Hartmann D, et al. Cell-matrix interaction via CD44 is independently regulated by different metalloproteinases activated in response to extracellular domain Ca^{2+} influx and PKC activation. J Cell Biol 2004;165:893–902.
25. Boutet P, Aguera-Gonzalez S, Atkinson S, et al. The metalloproteinase ADAM17/TNF-α enzyme regulates proteolytic shedding of the MHC class I-related chain B protein. J Immunol 2009;182:49–53.
26. Miyagi T, Takehara T, Tatsumi T, et al. CD1d-mediated stimulation of natural killer T cells selectively activates hepatic natural killer cells to eliminate experimentally disseminated hepatoma cells in murine liver. Int J Cancer 2003;106:81–9.

BH3-Only Protein Bid Participates in the Bcl-2 Network in Healthy Liver Cells

Hayato Hikita,[1*] Tetsuo Takehara,[1*] Takahiro Kodama,[1] Satoshi Shimizu,[1] Atsushi Hosui,[1] Takuya Miyagi,[1] Tomohide Tatsumi,[1] Hisashi Ishida,[1] Kazuyoshi Ohkawa,[1] Wei Li,[1] Tatsuya Kanto,[1] Naoki Hiramatsu,[1] Lothar Hennighausen,[2] Xiao-Ming Yin,[3] and Norio Hayashi[1]

Bcl-2 homology domain 3 (BH3)-only protein Bid is posttranslationally cleaved by caspase-8 into its truncated form (tBid) and couples with stress signals to the mitochondrial cell death pathway. However, the physiological relevance of Bid is not clearly understood. Hepatocyte-specific knockout (KO) of Bcl-xL leads to naturally-occurring apoptosis despite co-expression of Mcl-1, which shares a similar anti-apoptotic function. We generated Bcl-xL KO, Bcl-xL/Bid double KO, Bcl-xL/Bak double KO, Bcl-xL/Bax double KO, and Bcl-xL/Bak/Bax triple KO mice and found that hepatocyte apoptosis caused by Bcl-xL deficiency was completely dependent on Bak and Bax, and surprisingly on Bid. This indicated that, in the absence of Bid, Bcl-xL is not required for the integrity of differentiated hepatocytes, suggesting a complicated interaction between core Bcl-2 family proteins and BH3-only proteins even in a physiological setting. Indeed, a small but significant level of tBid was present in wild-type liver under physiological conditions. tBid was capable of binding to Bcl-xL and displacing Bak and Bax from Bcl-xL, leading to release of cytochrome c from wild-type mitochondria. Bcl-xL–deficient mitochondria were more susceptible to tBid-induced cytochrome c release. Finally, administration of ABT-737, a pharmacological inhibitor of Bcl-2/Bcl-xL, caused Bak/Bax-dependent liver injury, but this was clearly ameliorated with a Bid KO background. *Conclusion:* Bid, originally considered to be a sensor for apoptotic stimuli, is constitutively active in healthy liver cells and is involved in the Bak/Bax-dependent mitochondrial cell death pathway. Healthy liver cells are addicted to a single Bcl-2–like molecule because of BH3 stresses, and therefore special caution may be required for the use of the Bcl-2 inhibitor for cancer therapy. (HEPATOLOGY 2009;50:1972-1980.)

Bcl-2 family proteins regulate the mitochondrial pathway of apoptosis in mammalian cells.[1] They are divided into two basic groups: core Bcl-2 family proteins and Bcl-2 homology domain 3 (BH3)-only proteins. Core Bcl-2 family proteins have three or four Bcl-2 homology domains (BH1-BH4 domains), referred to as multidomain members, and structural similarity. These proteins display opposing bioactivities from inhibition to promotion of apoptosis and can be further divided into two groups: anti-apoptotic members, including Bcl-2, Bcl-xL, Bcl-w, Mcl-1, and Bfl-1, and pro-apoptotic members, including Bax and Bak. Pro-apoptotic Bak and Bax are effector molecules of the Bcl-2 family and induce release of cytochrome c from mitochondria, presumably through their ability to form pores at the mitochondrial outer membrane. Anti-apoptotic members, which serve as regulators, inhibit Bak and Bax. The original rheostat model argues for a fine balance between Bax-like pro-apoptotic proteins and Bcl-2–like an-

Abbreviations: ALT, alanine aminotransferase; BH3, Bcl-2 homology domain 3; KO, knockout; tBid, truncated form of Bid; TNF, tumor necrosis factor; TUNEL, terminal deoxynucleotidyl transferase-mediated 2'-deoxyuridine 5'-triphosphate nick-end labeling.

From the [1]Department of Gastroenterology and Hepatology, Osaka University Graduate School of Medicine, Osaka, Japan; [2]Laboratory of Genetics and Physiology, National Institute of Diabetes and Digestive and Kidney Diseases, National Institute of Health, Bethesda, MD; and the [3]Department of Pathology, University of Pittsburgh School of Medicine, Pittsburgh, PA.

[*]These authors contributed equally to this work and share first authorship.

Received May 20, 2009; accepted July 21, 2009.

Supported in part by a Grant-in-Aid for Scientific Research from the Ministry of Education, Culture, Sports, Science, and Technology, Japan (to T. Takehara).

Address reprint requests to: Norio Hayashi, M.D., Ph.D., Department of Gastroenterology and Hepatology, Osaka University Graduate School of Medicine, 2-2 Yamada-oka, Suita, Osaka 565-0871, Japan. E-mail: hayashin@gh.med.osaka-u.ac.jp; fax: (81)-6-6879-3629.

Copyright © 2009 by the American Association for the Study of Liver Diseases.

Published online in Wiley InterScience (www.interscience.wiley.com).

DOI 10.1002/hep.23207

Potential conflict of interest: Nothing to report.

Additional Supporting Information may be found in the online version of this article.

ti-apoptotic proteins in defining life and death, and this balance would be equal or favor survival in a healthy cell.[2]

BH3-only proteins consist of at least eight members and only share homology with each other and the core Bcl-2 family proteins through the short BH3 motif. They are transcriptionally induced or posttranslationally activated in response to a variety of apoptotic stimuli.[3] When they are induced or activated, they interact with core Bcl-2 family proteins and set the rheostat balance toward apoptosis by directly activating Bax-like molecules or neutralizing Bcl-2–like molecules.[4] Therefore, they serve as initial sensors of apoptotic signals that emanate from various cellular processes. Bid, a member of the BH3-only proteins, is activated via caspase-8–mediated cleavage in response to ligation of the death receptor, and its N-terminal truncated form (tBid) translocates to mitochondria and activates the mitochondrial death pathway.[5] In so-called type 1 cells, such as lymphoid cells, Fas activation leads to caspase-8 activation followed by direct activation of downstream caspases such as caspase-3 and caspase-7, where Bid dose not have significant roles.[6] In contrast, in type 2 cells, Fas-mediated activation of caspase-8 is not enough to activate downstream caspases. In those cells, tBid links the extrinsic or death-receptor pathway to the intrinsic or mitochondrial pathway to execute apoptosis. Hepatocytes are identified as a typical type 2 cell in which Bid plays a critical role in receptor-mediated cell death pathways.[7]

In our previous research, we found that genetic ablation of Bcl-xL in hepatocytes causes spontaneous apoptosis in mice.[8] This indicates that Bcl-xL is a critical apoptosis antagonist in adult healthy hepatocytes, although they possess other anti-apoptotic members of the Bcl-2 family such as Mcl-1. This might be simply explained by the fact that the absence of Bcl-xL affects the rheostat balance of core Bcl-2 family proteins by increasing the ratio of Bax and Bak to anti-apoptotic Bcl-2 proteins. Indeed, neuronal cell death during development caused by Bcl-xL deficiency is ameliorated by loss of Bax.[9] Platelet cell death caused by Bcl-xL deficiency is also ameliorated by loss of Bak.[10] These studies indicate that the stoichiometry between Bcl-xL and Bax or Bak dictates cellular fate. However, the possibility of BH3-only proteins being involved in the apoptosis rheostat in healthy cells has not been addressed. We generated Bcl-xL/Bid double-knockout (KO) mice and demonstrated that apoptosis caused by Bcl-xL deficiency is critically dependent on Bid. A small amount of Bid appears to be activated in the liver under physiological conditions and to be significant for inducing cytochrome c release from Bcl-xL–deficient mitochondria. This study shed light on the active participation of BH3-only proteins, which are generally considered to be sensors of apoptotic stimuli, in the Bcl-2 network regulating life and death of healthy differentiated hepatocytes.

Materials and Methods

Mice. Mice carrying a *bcl-x* gene with 2 *lox*P sequencers at the promoter region and a second intron ($bcl\text{-}x^{flox/flox}$) were described previously.[11] Heterozygous AlbCre transgenic mice expressing Cre recombinase gene under the promoter of the albumin gene[8] and traditional Bid KO mice[7] also have been described previously. We purchased from the Jackson Laboratory (Bar Harbor, ME) traditional Bak KO mice, traditional Bax KO mice, and conditional Bak/Bax KO mice ($bak^{-/-}$ $bax^{flox/flox}$).[12] We generated hepatocyte-specific Bcl-xL KO mice ($bcl\text{-}x^{flox/flox}$ *AlbCre*), Bcl-xL/Bid double-KO mice ($bid^{-/-}$ $bcl\text{-}x^{flox/flox}$ *AlbCre*), Bcl-xL/Bak double-KO mice ($bak^{-/-}$ $bcl\text{-}x^{flox/flox}$ *AlbCre*), Bcl-xL/Bax double-KO mice ($bax^{-/-}$ $bcl\text{-}x^{flox/flox}$ *AlbCre*), and Bcl-xL/Bak/Bax triple-KO mice ($bak^{-/-}$ $bax^{flox/flox}$ $bcl\text{-}x^{flox/flox}$ *AlbCre*) by mating the strains. They were maintained in a specific pathogen-free facility and treated with humane care under approval from the Animal Care and Use Committee of Osaka University Medical School.

Apoptosis Assay. The levels of serum alanine aminotransferase (ALT) were measured by a standard method, and serum caspase-3/7 activity was measured by a luminescent substrate assay for caspase-3 and caspase-7 (Caspase-Glo assay, Promega, Tokyo, Japan). The caspase-3/7 activity was normalized by each control group. For histological analysis, the liver sections were stained with hematoxylin-eosin. To detect cells with oligonucleosomal DNA breaks, the sections were also subjected to terminal deoxynucleotidyl transferase-mediated deoxyuridine triphosphate nick-end labeling (TUNEL) staining, according to a previously reported procedure.[13]

Western Blot Analysis. Liver tissue was lysed with a lysis buffer (1% Nonidet P-40, 0.5% sodium deoxycholate, 0.1% sodium dodecyl sulfate, 1 × protein inhibitor cocktail (Nacalai tesque, Kyoto, Japan), phosphate-buffered saline, pH 7.4). Equal amounts of protein were electrophoretically separated by sodium dodecyl sulfate polyacrylamide gels and transferred onto polyvinylidene fluoride membrane. For immunodetection, the following antibodies were used: anti-Bcl-xL antibody (Santa Cruz Biotechnology, Santa Cruz, CA), anti-Mcl-1 antibody (Rockland, Gilbertsville, PA), previously described anti-Bid antibody generated from glutation-S-transferase-Bid fusion protein,[14] anti-full-length Bid antibody, anti-cleaved caspase-7 antibody, anti-Bax antibody, anti-Cox IV antibody (Cell Signaling Technology, Beverly, MA),